Faraday Discuss., 1994, **97**, 415–452

GENERAL DISCUSSION

Prof. Dagdigian opened the discussion of Prof. Heaven's paper: We† would like to amplify the discussion given by you on the expected bender levels for NeCH($X\,^2\Pi$) and to present recent calculations on the related system ArCH($X\,^2\Pi$), which has been studied experimentally by Lemire *et al.*[1]

The lowest rotational asymptote for NeCH($X\,^2\Pi$) is CH($j = 1/2$, F_2) + Ne. Because of the two-fold orbital and $2j + 1$ spatial degeneracy, there will be four bender curves correlating with this asymptote. In the notation of Dubernet *et al.*[2] these can be identified as $P = 1/2$, $\xi = \pm 1$ and $P = -1/2$, $\xi = \pm 1$ (all with $\omega = 1/2$). Alternatively, by taking symmetrized diatom rotational basis functions, as in our recently described body-frame (BF) basis,[3,4] we would describe the bender curves as $P = 1/2$, $\varepsilon = +1$, $\xi = \pm 1$ and $P = 1/2$, $\varepsilon = -1$, $\xi = \pm 1$. We can consider the splittings between these bender curves induced by various terms in the Ne–CH($X\,^2\Pi$) interaction potential. In the absence of rotation, the V_2 term alone does not induce a splitting between these levels. As you note the Coriolis term does cause a splitting whose magnitude increases with increasing J; however, the levels still appear as doubly degenerate pairs, of total parity $\pi = \pm 1$. Inclusion of the V_1 term causes a splitting between these pairs, even in the absence of rotation. The spectra reported by you are consistent with the presence of either two sets of doubly degenerate pairs of $P = 1/2$ levels, as you have assumed, or a single nearly degenerate pair of $P = 1/2$ rotational levels in the ground vibrational level of NeCH($X\,^2\Pi$).

Because of the orbital degeneracy of CH($X\,^2\Pi$), two potential-energy surfaces (PESs), of A′ and A″ symmetry, are required to describe the interaction of this diatom with a rare-gas atom; these surfaces differ in the orientation of the unpaired π electron with respect to the triatomic plane. For the intensively studied ArOH($X\,^2\Pi$) complex, with a $\sigma^2\pi^3$ electron occupancy, the difference (V_{dif}) in the A′ and A″ PESs is small.[5] Similarly, you have assumed that V_{dif} is small and can be neglected for NeCH($X\,^2\Pi$). By contrast, in our collaborative theoretical[3] and experimental[6] study of ArBH($A\,^1\Pi$), with a $\sigma\pi$ electron occupancy, we find that V_{dif} is comparable in magnitude to the diatom rotational spacings and therefore must be included explicitly in the calculation of bender energies.

We have also recently computed[7] multi-reference, configuration–interaction potential-energy surfaces and, subsequently, the bend–stretch energies for ArCH($X\,^2\Pi$), in order to provide a detailed interpretation of the experiments of Lemire *et al.*,[1] who observed the electronic transition between the $X\,^2\Pi$ and $B\,^2\Sigma^-$ states of ArCH. As for ArBH($A\,^1\Pi$), we find that V_{dif} is large for the ArCH($X\,^2\Pi$) complex, which has a $\sigma^2\pi$ electron occupancy. The separation between the lowest two sets of $P = 1/2$ degenerate pairs of levels is comparable to the energy separation between the lowest Ar–CH rotational asymptotes.

Our *ab initio* calculations, compared with those of Degli-Esposti and Werner for ArOH,[5] suggest that V_{dif} will be large for Ar–diatomic hydride complexes in Π electronic states in which the electronic state of the diatomic moiety corresponds to a singly filled π orbital but much smaller when the electronic state of the diatomic has a triply filled π orbital.

Green and Lester[8] have shown that the degenerate pairs of $P = 1/2$ levels of the same J will exhibit a parity splitting variety as $p(J + 1/2)$, where the splitting constant p will be directly proportional to V_{dif} averaged over the Van der Waals stretch wavefunction. This splitting is analogous to that expected for a $K = 0$ vibronic level of a linear

† P. J. Dagdigian and M. H. Alexander.

triatomic Renner–Teller $^2\Pi$ linear triatomic molecule, for which Hougen[9] has shown that p can vary from $-2B$ to $+2B$. When the magnitude of p is small, the pattern of Van der Waals rotational levels will behave similarly to a case (a) $\Omega = 1/2$ manifold, as you have observed for NeCH($X\,^2\Pi$). By contrast, a large parity splitting was found for ArCH($X\,^2\Pi$),[2] and the rotational levels had the same pattern as that for a case (b) $^2\Sigma$ state. Our recent calculations on ArCH($X\,^2\Pi$), which will be described in detail elsewhere,[7] reproduce quite closely the experimentally observed parity splittings.

Similar *ab initio* calculations on NeCH($X\,^2\Pi$) indicate that V_{dif} is not small. Further work on NeCH needs to be carried out to ascertain what information the experimental spectrum can provide about the magnitude of V_{dif}.

1 G. W. Lemire, M. J. McQuaid, A. J. Kotlar and R. C. Sausa, *J. Chem. Phys.*, 1993, **99**, 91.
2 M-L. Dubernet, D. Flower and J. M. Hutson, *J. Chem. Phys.*, 1991, **94**, 7602.
3 M. H. Alexander, S. Gregurick and P. J. Dagdigian, *J. Chem. Phys.*, 1994, **101**, 2887.
4 P. J. Dagdigian and M. H. Alexander, *Faraday Discuss.*, 1994, **98**, 417.
5 A. Degli-Esposti and H-J. Werner, *J. Chem. Phys.*, 1990, **93**, 3351.
6 E. Hwang and P. J. Dagdigian, *J. Chem. Phys.*, 1994, **101**, 2903.
7 M. H. Alexander, S. Gregurick, P. J. Dagdigian, G. W. Lemire, M. J. McQuaid and R. C. Sausa, *J. Chem. Phys.*, 1994, **101**, in the press.
8 W. H. Green Jr. and M. I. Lester, *J. Chem. Phys.*, 1992, **96**, 2573.
9 J. T. Hougen, *J. Chem. Phys.*, 1962, **36**, 519.

Prof. Heaven replied: In responding to your comments, it will be helpful to clarify a significant point. In our analysis of the Ne–CH spectrum we identified transitions arising from the two 'bending' states that correlate with CH($X\,^2\Pi_{1/2}$, $j = 1/2$). Using the body-fixed quantum numbers defined by Dubernet *et al.*,[1] the $\omega = \pm 1/2$, $j = 1/2$ states of the diatom become $P = -1/2$ and $P = 1/2$ bending states of the complex. Both of these states possess two levels of opposite parity for each value of J. The $P = -1/2$ and $P = 1/2$ states may be pushed apart by terms arising from both the average (V_Π) and difference (V_d) potentials. From the spectroscopic data we deduced that the $P = -1/2$ and $P = 1/2$ states of Ne–CH($X\,^2\Pi_{1/2}$, $j = 1/2$) are separated by *ca.* 5 cm^{-1}. Hence the rotational structures of the bands (*e.g.* Fig. 2 of our paper) were attributed to transitions from nearly degenerate pairs of levels (parity doublets) belonging to individual $P = -1/2$ or $P = 1/2$ states.

We modelled the $P = -1/2 \leftrightarrow P = 1/2$ splitting by considering the effects of the average potential. Although the difference potential was not included, we did not assume that it was insignificant. As you note, the difference potential is also capable of splitting the $P = \pm 1/2$ states apart. We have recently calculated *ab initio* potential-energy surfaces for Ne–CH.[2] These calculations provide average and difference potentials that are of comparable magnitude for the typical Ne–CH distance of 3.8 Å. Angular cuts through the potentials, taken at this radius, are dominated by $P_2^0(\cos\theta)$ (average potential) and $P_2^2(\cos\theta)$ (difference potential) terms. Using the bending–rotation model outlined in our paper we can reproduce the observed ground-state energy levels with $V_\Pi = 20P_2^0(\cos\theta)$ and $V_d = -8.7P_2^2(\cos\theta)$ cm^{-1}.

Our intention in studying the effects of the average potential alone was to explore possible causes for the occurrence of integer rotational quantum numbers for ground-state Ar–CH($X\,^2\Pi_{1/2}$, $j = 1/2$).[3] We found that, under specific circumstances, integer quantum numbers could be observed without assuming that the spin–orbit coupling had been quenched. Alexander, Dagdigian and co-workers have recently calculated *ab initio* surfaces for Ar–CH(X).[4] They computed rovibronic energy levels from these surfaces, and concluded that the spin–orbit coupling of the diatom must be quenched in order to obtain agreement with experiment. We have briefly explored the predictions of our bending–rotation model using approximate angular potentials based on the *ab initio* surfaces.[4] The primitive potentials $V_\Pi = 100P_2^0(\cos\theta)$ and $V_d = -45P_2^2(\cos\theta)$ yielded levels characterized by integer rotational quantum numbers (N). However, the splittings

between the $J = N + 1/2$ and $J = N - 1/2$ levels were overestimated. In these calculations the spin–orbit coupling constant was held at the unperturbed value of 27 cm^{-1}. Reduction of this constant to around 10 cm^{-1} gave fine-structure splittings that were in agreement with experiment.

To summarize, you emphasized the importance of the difference potential in determining the energy level structures of Rg–CH(X) complexes. We are in full agreement with this view. Preliminary calculations indicate that qualitatively similar potentials can account for the ground-state structures of Ne–CH(X) and Ar–CH(X). For Ne–CH(X), the spectrum can be reproduced without assuming that the spin–orbit coupling has been perturbed. The levels of Ar–CH(X) can also be represented by models that retain the unperturbed diatomic spin–orbit coupling constant, but the potentials implied by these models are qualitatively different from those of Ne–CH(X), and inconsistent with the results from *ab initio* calculations. Hence, it appears that the stronger interaction with Ar is sufficient to produce a measurable quenching of the spin–orbit coupling in CH(X).

We thank you for your valuable comments, and for sharing your results on Ar–CH prior to publication.

1 M-L. Dubernet, D. Flower and J. M. Hutson, *J. Chem. Phys.*, 1991, **94**, 7602.
2 U. Schnupf, K. Morokuma and M. C. Heaven, work in progress.
3 G. W. Lemire, M. J. McQuaid, A. J. Kotlar and R. C. Sausa, *J. Chem. Phys.*, 1993, **99**, 91.
4 M. H. Alexander, S. Gregurick, P. J. Dagdigian, G. W. Lemire, M. J. McQuaid and R. C. Sausa, *J. Chem. Phys.*, 1994, **101**, in the press.

Prof. Dagdigian and **Prof. Alexander** commented: In their analysis of the electronic spectra of the CH/D–Ne and ArOH, Prof. Heaven and Prof. Lester have employed the body-frame (BF) basis functions defined by Dubernet *et al.*,[1] who have provided a very useful pedagogic general discussion of the vibrational energy level structure of Van der Waals complexes of open-shell diatomic free radicals. We have proposed[2] the use of a slightly different BF basis, which has also found utility[3] for the calculation, within the centrifugal decoupling approximation,[4] of bimolecular state-to-state rotationally inelastic cross-sections involving diatomic free radicals.

We can expand the wavefunction of the Van der Waals complex as follows:

$$\Psi^{JM} = (1/R) \sum_{jP\Omega\varepsilon} C^{JM}_{jP\Omega\varepsilon}(\boldsymbol{R}) \,|\, jP\Omega\varepsilon;\, JM\rangle \tag{1}$$

where J designates the total angular momentum with space-fixed projection M. Here the usual Jacobi coordinate $\boldsymbol{R}$ denotes the orientation of the vector connecting the diatom centre of mass and the rare-gas atom. In this equation we have assumed, for simplicity, that the vibrational motion of the diatomic is frozen. This could be added without any loss of generality in the argument that follows. In eqn. (1) the quantities j, Ω and ε refer to the diatom moiety and denote, respectively, the angular momentum, its projection on the internuclear axis, and e/f symmetry[5] index of the rotational/fine-structure states of the diatom [$\varepsilon = +1$ for the e-labelled and $\varepsilon = -1$ for the f-labelled diatomic states[6]]. We have followed the notation of Dubernet *et al.*[3] and denoted as P the projection of the total angular momentum (inclusive of spin) on the diatom–rare gas intermolecular axis.

The BF basis functions in eqn. (1) can be written as

$$|\, jP\Omega\varepsilon;\, JM\rangle = 2^{-1/2}[\,|\, jP\Omega;\, JM\rangle + \varepsilon\,|\, jP, -\Omega; JM\rangle] \tag{2}$$

where the signed-Ω BF functions are given by[3]

$$|\, jP\Omega;\, JM\rangle = \frac{[(2j+1)(2J+1)]^{1/2}}{4\pi} D^{J*}_{M,\,P}(\hat{R}) D^{j*}_{P,\,\Omega}(\hat{r}_b)\,|\, \Lambda\Sigma\rangle \tag{3}$$

where $\hat{r}_b$ denotes the orientation of the diatom internuclear axis P in the body frame. Because the signed-P BF basis functions in eqn. (2) do not have well defined parity for $P \neq 0$, we define states of definite parity as follows:

$$|jP\varepsilon\xi; JM\rangle = 2^{-1/2}[|jP\varepsilon; JM\rangle + \xi|j, -P\varepsilon; JM\rangle] \quad (4)$$

where we have introduced the additional symmetry index $\xi = \pm 1$. In the absence of Coriolis coupling, for a given (positive) value of P, the eigenfunctions appear to degenerate pairs. The parity ($\pi = \pm 1$) of the $|jP\varepsilon\xi; JM\rangle$ functions in eqn. (4) is $\varepsilon\xi(-1)^{J-S+s}$, where S is the total electron spin, and s equals 1 for a diatomic Σ^- state and 0 otherwise. We can define the e and f levels[5] of the complex as those for which $\varepsilon\xi(-1)^s = +1$ and -1, respectively.

The present BF basis differs from that chosen by Dubernet *et al.*,[1] who define and label their basis functions by the sign of the product $P\Omega$. This is equivalent to employing the signed-Ω functions $|jP\Omega; JM\rangle$ instead of the symmetrized functions $|jP\varepsilon; JM\rangle$ in eqn. (4). We prefer the present BF basis since the symmetrization of the diatom wavefunction in eqn. (2) brings the diatomic rotational fine-structure Hamiltonian[7] closer to a diagonal form. Indeed, for diatoms in singlet spin multiplicity states, it is already diagonal. Moreover, for complexes involving diatoms in Π electronic states for which there is a large difference (V_{dif}) in the interaction potential when the unpaired π electron lies in or perpendicular to the triatomic plane, the wavefunctions are not well characterized by the product $P\Omega$, unlike the situation when V_{dif} is small.[1] The interaction V_{dif} breaks the cylindrical symmetry of the interaction potential since this term couples[6] different Ω states ($\Delta\Omega = \pm 2$). Consequently, the symmetric and antisymmetric combinations of the $\pm\Omega$ states are a more appropriate basis.

The utility of our BF basis is perhaps best exemplified for Van der Waals complexes of atoms in $^1\Pi$ states, *e.g.* ArBH($A\,^1\Pi$), about which we have presented, in the poster session at this Discussion, a contribution on our experimental[8] and theoretical[2] work. Consider explicitly the bender curves correlating with the lowest rotational asymptote, *i.e.* BH($A\,^1\Pi$, $j = 1$)–Ar. Because of the two-fold orbital and $2j + 1$ spatial degeneracy, there will be six such bender curves, three of each parity:

$\pi = +1$		$\pi = -1$	
(1)	$P = 0, \varepsilon = +1,$	(4)	$P = 0, \varepsilon = -1,$
(2)	$P = 1, \varepsilon = +1, \xi = +1,$	(5)	$P = 1, \varepsilon = +1, \xi = -1,$
(3)	$P = 1, \varepsilon = -1, \xi = -1,$	(6)	$P = 1, \varepsilon = -1, \xi = +1.$

In the absence of Coriolis coupling, the pairs of functions {(2),(5)} and {(3),(6)} will be degenerate. When V_{dif} is large, as it is for ArBH($A\,^1\Pi$),[2] the two $P = 0$ levels [(1) and (4)] will be separated significantly in energy, as will the two $P = 1$ (nominally) degenerate pairs {[(2),(5)] and [(3),(6)]}. In the labelling scheme of Dubernet *et al.*[1] the two $P = 0$ levels would be the sum and difference of states (1) and (4), which would be strongly coupled by the difference term (V_{dif}) in the interaction potential. The different character of the two $P = 0$ levels is analogous to the case (c) $\Omega = 0^+$ and $\Omega = 0^-$ states of a diatomic molecule.[9] Also, the electronic spectrum of the ArBH Van der Waals complex provides a dramatic illustration of this difference: radiative transitions from the ground vibrational level of ArBH($X\,^1\Sigma^+$) are allowed to the $\varepsilon = +1$ level, but forbidden to $\varepsilon = -1$.[2,8]

In our recently completed experimental study[8] of ArBH, and further experiments on the analogous ArAlH complex,[10] laser fluorescence spectra have been recorded for a number of rotationally resolved and diffuse bands of these complexes in the vicinity of the $A\,^1\Pi \leftarrow X\,^1\Sigma^+$ (0,0) band of the diatomic hydride. The Van der Waals complexes were prepared in a pulsed jet by 193 nm photolysis of diborane (for ArBH) and trimethylaluminum (for ArAlH) seeded in a Ar–He mixture. Both perpendicular [$P' = 1 \leftarrow P'' = 0$] and parallel [$P' = 0 \leftarrow P'' = 0$] transitions have been observed, and

the upper-state rotational constants for the various bend–stretch levels vary by more than a factor of 2. The pattern of bend–stretch vibrational energies is complicated, and stretch levels supported by different bender curves are interleaved among each other.

In order to provide an incisive interpretation of these experimental results, we have computed multi-reference, configuration–interaction potential-energy surfaces and, subsequently, the bend–stretch energies for ArBH($X\,^1\Sigma^+$, $A\,^1\Pi$).[2] Similar calculations have been performed for ArAlH.[11] For the $A\,^1\Pi$ electronic state, the diatom is in an orbitally degenerate state, and the approach of the rare-gas partner leads to two potential-energy surfaces, of A′ and A″ symmetry. Unlike the situation for ArOH($X\,^2\Pi$)[12] and ArNO($X\,^2\Pi$),[13] the differences between the A′ and A″ PESs are large and cannot be treated as a perturbation. The most strongly bound ArBH($A\,^1\Pi$) states, with Ar–BH separations less than in the ground bend–stretch level of ArBH($X\,^1\Sigma^+$), correspond to motion primarily on the more attractive A″ PES, with a minimum in approximately T-shaped geometry. The calculated ArBH($A\,^1\Pi$) bend–stretch energies[2] have been used to provide unambiguous assignments for the first ten observed bands in the experimental ArBH spectrum.[8] The large difference in experimental rotational constants for the upper states reflects, in large part, the large differences in the equilibrium Ar–BH separations for the various bender curves. As expected from our derived spectroscopic selection rule,[2,8] discussed above, transitions from the ground bend–stretch level of ArBH($X\,^1\Sigma^+$) to bend–stretch levels supported by the lowest ArBH($A\,^1\Pi$) bender curve [$P = 0$, $\varepsilon = -1$] were not observed.[8]

1 M-L. Dubernet, D. Flower and J. M. Hutson, *J. Chem. Phys.*, 1991, **94**, 7602.
2 M. H. Alexander, S. Gregurick and P. J. Dagdigian, *J. Chem. Phys.*, 1994, **101**, 2887.
3 See, for example, G. C. Corey and M. H. Alexander, *J. Chem. Phys.*, 1986, **85**, 5652.
4 D. J. Kouri, in *Atom–Molecule Collision Theory: A Guide for the Experimentalist*, ed. R. B. Bernstein, Plenum, New York, 1979, p. 301.
5 J. M. Brown, J. T. Hougen, K-P. Huber, J. W. C. Johns, I. Kopp, H. Lefebvre-Brion, A. J. Merer, D. A. Ramsay, J. Rostas and R. N. Zare, *J. Mol. Spectrosc.*, 1975, **55**, 500.
6 M. H. Alexander, *Chem. Phys.*, 1985, **92**, 337.
7 H. Lefebvre-Brion and R. W. Field, *Perturbations in the Spectra of Diatomic Molecules*, Academic, New York, 1986.
8 E. Hwang and P. J. Dagdigian, *J. Chem. Phys.*, 1994, **101**, 2903.
9 G. Herzberg, *Spectra of Diatomic Molecules*, Van Nostrand, Princeton, 2nd edn., 1968.
10 E. Hwang and P. J. Dagdigian, *J. Chem. Phys.*, submitted.
11 M. Yang, M. H. Alexander, S. Gregurick and P. J. Dagdigian, *J. Chem. Phys.*, submitted.
12 A. Degli-Esposti and H-J. Werner, *J. Chem. Phys.*, 1990, **93**, 3351.
13 M. H. Alexander, *J. Chem. Phys.*, 1993, **99**, 7725.

Dr. Hutson said: There are many different basis sets that can be used in discussing the energy levels of Van der Waals complexes. In our work on the coupling cases that may be observed in complexes containing open-shell molecules,[1] we developed a body-fixed basis set with functions labelled by quantum numbers P and ω (Ω in Prof. Dagdigian's notation), which are the projections of J onto the intermolecular axis and of the diatom j onto the diatom axis. We then noted that the $P_1(\cos\theta)$ anisotropy has diagonal matrix elements that depend on the relative sign of P and ω. We thus proposed that it was most convenient to use basis functions labelled by this relative sign and to define the parity-symmetrised basis functions by

$$2^{-1/2}[|jP\omega;\, JM\rangle + \varepsilon|j - P - \omega;\, JM\rangle]$$

so that they combine functions that are degenerate with respect to the odd-order potential anisotropies. We termed this the signed-ω basis set. Our model has been very successful in interpreting the spectra of complexes such as Ar–OH ($X\,^2\Pi$), where there can be no doubt that the real eigenstates are similar in character to the signed-ω basis functions.

Prof. Dagdigian has suggested the use of an alternative basis set, in which the monomer functions $|j\omega\rangle$ are symmetrised before multiplying them by overall rotational

functions. This is of course the standard approach in scattering theory, because the properly symmetrised asymptotic monomer wavefunctions appear explicitly in this basis set. Indeed, this is the approach that we adopted when we began our original work, but we decided in the end that it gave a less transparent description of the eigenstates for systems such as Ar–OH. Its disadvantage is that there are matrix elements involving the odd-order anisotropies that connect the functions with $\varepsilon = \pm 1$, and for many systems (including Ar–OH) these are much larger than the difference between the diagonal matrix elements.

As Prof. Dagdigian has mentioned, there are other parts of the Hamiltonian that are diagonal in his basis set but off-diagonal in ours. These include the monomer λ-doubling terms and, for the special case of a diatomic molecule in a state with $\omega = 1$, the difference terms in the interaction potential. For spectroscopic understanding, it is usually most illuminating to use a basis set that gives a Hamiltonian matrix as diagonal as possible. Thus different basis sets will be appropriate in different cases:

(1) Our signed-ω basis set is appropriate when the main splittings in the spectrum are due to the odd-order [principally $P_1(\cos\theta)$] terms in the sum potential;

(2) Prof. Dagdigian's symmetrised basis set is appropriate when the splittings due to the odd-order anisotropies are swamped by those due to either (i) the monomer λ doubling or (ii) the difference potential. In particular, this occurs for $P = 0$ states with $\omega = 1$, where the splittings due to odd-order anisotropies vanish. It will also occur for complexes of homonuclear diatomic molecules, where the odd-order anisotropies are zero.

The choice of basis set is thus very much a matter of 'horses for courses'. There is no single 'best' basis set for all systems and all purposes. For exact calculations, where all the basis functions are included, the choice of basis set does not affect the results, and one simply chooses the set for which the matrix elements are easiest to evaluate. However, for approximate calculations, or when trying to assign appropriate quantum numbers to observed energy levels, the choice of basis set does make a difference.

1 M-L. Dubernet, D. Flower and J. M. Hutson, *J. Chem. Phys.*, 1991, **94**, 7602.

Dr. M-L. Dubernet said: We have developed potential-energy surfaces[1] for the ground state of Ar–OH by fitting to high-resolution spectroscopy. We used the SEP results of Lester and co-workers[2] for bending and stretching frequencies, rotational constants and the parity splitting of the first excited bending state ($P = 1/2$). The ground-state ($P = 3/2$) rotational constant determined by Endo and co-workers[3] was included.

As expected, we obtained an average potential $V_{\Pi}(R, \theta)$ considerably deeper than the *ab initio* potential,[4] with a lower barrier to internal rotation. As mentioned in the paper by Endo and co-workers, the difference potential $V_2(R, \theta)$ has a strong influence on the parity splittings. Simple perturbative models[5,6] make it difficult to reconcile the experimental value of the microwave ground-state parity splitting with the bending frequencies and parity splittings from the SEP spectra.

Despite extensive efforts, we have been unable to find a physically acceptable potential that reproduces the parity splittings for both the $P = 1/2$ and $P = 3/2$ states. It would thus be very valuable to have rotationally resolved spectra for further excited bending and stretching levels. It would also be very helpful to obtain unambiguous assignments of the $\omega = 1/2$ states, since the pattern of these is important in determining the ground-state parity splitting.[6]

1 M-L. Dubernet and J. M. Hutson, *J. Chem. Phys.*, 1993, **99**, 7477.
2 M. T. Berry, R. A. Loomis, L. C. Giancarlo and M. I. Lester, *J. Chem. Phys.*, 1992, **96**, 7890.
3 Y. Ohshima, M. Iida and Y. Endo, *J. Chem. Phys.*, 1991, **95**, 7001.
4 A. Degli Esposti and H. J. Werner, *J. Chem. Phys.*, 1990, **93**, 3351.
5 W. H. Green and M. I. Lester, *J. Chem. Phys.*, 1992, **96**, 2573.
6 M-L. Dubernet, P. A. Tuckey and J. M. Hutson, *Chem. Phys. Lett.*, 1992, **193**, 355.

Prof. Lester replied: You reported that you and Dr. Hutson[1] had developed potential-energy surfaces for the ground state of Ar–OH based on the stimulated emission pumping results from this laboratory.[2,3] We have also carried out a non-linear least-squares fitting procedure to construct a potential-energy surface for OH ($X\,^2\Pi$) + Ar which is consistent with experimental measurements of the intermolecular energy levels from 0–89 cm^{-1} and rotor constants for OH–Ar ($X\,^2\Pi$).[4] This procedure is more complicated for OH–Ar ($X\,^2\Pi$) than for closed-shell systems,[5] since two potential-energy surfaces, the A′ and A″ surfaces, correlate with OH ($X\,^2\Pi$) + Ar. The A′ and A″ surfaces differ in the orientation of the unpaired electron of the OH radical with respect to the OH–Ar plane. Previous theoretical calculations have shown that the energies of the intermolecular vibrational levels were determined essentially by the average potential, $V_\Pi = (V_{A'} + V_{A''})/2$.[6] On the other hand, the primary effect of the difference potential, $V_2 = (V_{A''} - V_{A'})/2$, was to induce parity splittings in the rotational level structure.[6,7] Since our goal was to improve the fit of calculated to experimental values for the bound intermolecular bending and stretching levels, we have varied only the average V_Π potential and held the difference potential fixed at its *ab initio* value.[8] This differs from your procedure where you have attempted to determine V_Π and V_2 simultaneously. We used the *ab initio* average potential as the initial guess in our fitting procedure; the details are given elsewhere.[4]

The average intermolecular potential for OH ($X\,^2\Pi$) + Ar obtained in the least-squares fitting procedure is shown as a contour plot in Fig. 1. The potential minimum of -127 cm^{-1} occurs at an OH (centre-of-mass) to Ar separation (R) of 3.7 Å in the linear

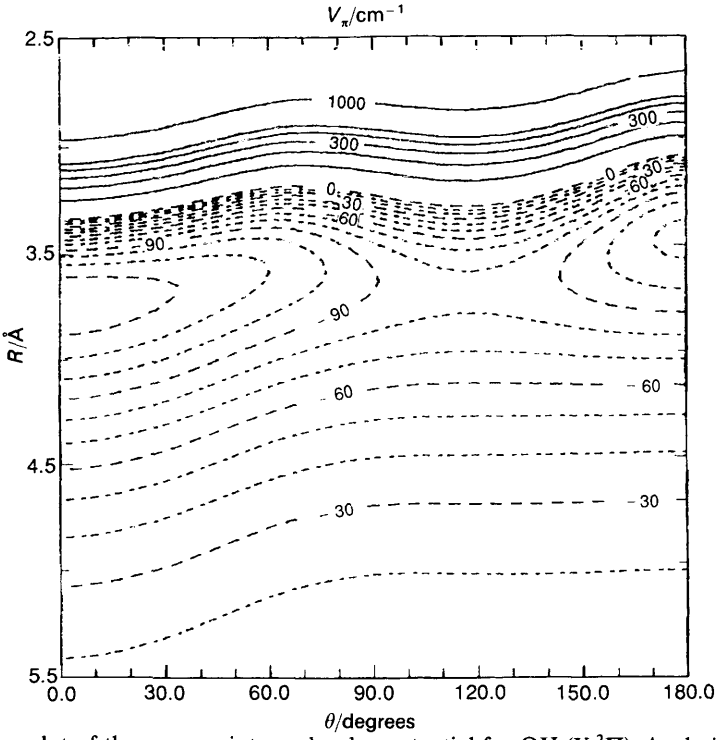

Fig. 1 Contour plot of the average intermolecular potential for OH ($X\,^2\Pi$)–Ar derived in a least-squares fitting procedure from the experimentally observed vibrational energy levels from 0–89 cm^{-1}. In the attractive well region (dashed contour lines), contours are shown at 10 cm^{-1} intervals. Along the repulsive wall (solid contour lines), contours are drawn at 100 cm^{-1} intervals from 0–500 cm^{-1}. $\theta = 0°$ corresponds to the linear O—H–Ar configuration.

O—H–Ar geometry ($\theta = 0°$). The barrier to internal rotation is 45 cm^{-1} and is located at $R = 3.7$ Å and $\theta \approx 120°$. A secondary minimum with a well-depth of -113 cm^{-1} is found at the linear H—O–Ar configuration ($\theta = 180°$) at a slightly shorter bond length of 3.5 Å. The bound states supported by this empirically adjusted potential agree within *ca.* 2% of the experimental vibrational energies. Our fitted potential is in good accord with the V_{Π} potential derived by Dubernet and Hutson[1] which has a well-depth of -126 cm^{-1} in a near-linear Ar–O—H geometry and a barrier to internal rotation of 44 cm^{-1}.

The lowest intermolecular energy level is computed to have a binding energy of 93.2 cm^{-1} with respect to the OH ($X\,^2\Pi_{3/2}$) $j = 3/2$ + Ar asymptote. The magnitude of the calculated binding energy is within the experimental limits, $93 \leqslant D_0/cm^{-1} \leqslant 94.2$, deduced from the appearance of OH $A\,^2\Sigma^+$ ($v = 0$, $n = 0$) products upon electronic excitation of OH–Ar in the A–X 0–0 region[9] and the onset of bound-free transitions in stimulated emission pumping spectra,[3] but it is much greater than the 65 cm^{-1} predicted from an *ab initio* calculation of the OH ($X\,^2\Pi$) + Ar potential.[6] Dubernet and Hutson obtain a binding energy of 95.5 cm^{-1} from their fit.[1] The well-depth of our empirically adjusted potential is *ca.* 25% greater than the *ab initio* potential.[8] A closer comparison of the *ab initio* and least-squares derived potentials reveals that the *ab initio* isotropic attraction is too weak by *ca.* 50%. Smaller, but significant, discrepancies are found in the anisotropic terms. The fitted potential exhibits a deeper secondary minimum at $\theta = 180°$ than does the *ab initio* surface.

1 M-L. Dubernet and J. M. Hutson, *J. Chem. Phys.*, 1993, **99**, 7477.
2 M. T. Berry, M. R. Brustein, M. I. Lester, C. Chakravarty and D. C. Clary, *Chem. Phys. Lett.*, 1991, **178**, 301.
3 M. T. Berry, R. A. Loomis, L. C. Giancarlo and M. I. Lester, *J. Chem. Phys.*, 1992, **96**, 7890.
4 M. I. Lester, W. H. Green Jr., C. Chakravarty and D. C. Clary, in *Molecular Dynamics and Spectroscopy by Stimulated Emission Pumping*, ed. H-L. Dai and R. W. Field, World Scientific, Singapore, 1994.
5 J. M. Hutson, *Annu. Rev. Phys. Chem.*, 1990, **41**, 123.
6 C. Chakravarty and D. C. Clary, *J. Chem. Phys.*, 1991, **94**, 4149.
7 W. H. Green Jr. and M. I. Lester, *J. Chem. Phys.*, 1992, **96**, 2573.
8 A. Degli Esposti and H-J. Werner, *J. Chem. Phys.*, 1990, **93**, 3351.
9 L. C. Giancarlo, R. W. Randall, S. E. Choi and M. I. Lester, *J. Chem. Phys.*, 1994, **101**, 2914.

Prof. Lester opened the discussion of Prof. Endo's paper: You and your co-workers, both here and in ref. 1, have reported the pure rotational spectrum of OH–Ar by applying Fourier-transform microwave spectroscopy. Parity splittings have been measured for the lowest two pure rotational transitions ($J = 7/2$–$5/2$ and $J = 5/2$–$3/2$) of the ground bending state ($j = 3/2$, $\omega = 3/2$, $P = 3/2$) of OH–Ar. These splittings between rotational levels with the same total angular momentum but opposite parity, called parity splitting or *P*-doubling, are a sensitive probe of the intermolecular potential in open-shell systems such as OH–Ar ($X\,^2\Pi$).

Bound-state calculations performed by Chakravarty and Clary[2] based on an *ab initio* potential for OH ($X\,^2\Pi$)–Ar[3] predicted an extremely small parity splitting for the lowest bending state of OH–Ar ($j = 3/2$, $\omega = 3/2$, $P = 3/2$) and a significantly larger parity splitting (*ca.* 0.43 cm^{-1} at $J = 3/2$) for the first excited intermolecular level with $j = 3/2$, $\omega = 3/2$, $P = 1/2$. The calculations showed conclusively that the parity splittings originate from the difference potential, $V_2 = (V_{A''} - V_{A'})/2$, since splittings were not evident when this term in the Hamiltonian was turned off. The difference potential reflects the dependence of the intermolecular potential on the orientation of the orbital containing the OH unpaired electron. The A′ and A″ surfaces correspond to this orbital lying in or out of the OH–Ar plane, respectively.

Using the stimulated emission pumping (SEP) technique, Berry *et al.*[4,5] have accessed virtually all of the bound states supported by OH ($X\,^2\Pi$) + Ar potential as well as many predissociative levels which lie above the dissociation limit. As predicted by the theoretical calculations, the first excited intermolecular vibrational band at 9.7 cm^{-1},

assigned as $j = 3/2$, $\omega = 3/2$, $P = 1/2$, $v_s = 0$, exhibited a noticeable parity splitting. The spacings between parity doublets were quite large, comparable to the energy spacings between rotational levels of the complex. Since Q_1 transitions always terminate on the lower-energy component of the parity doublet while P_1 and R_1 transitions always terminate on the higher energy component, the parity splitting results in a gross shift of the Q_1 branch relative to the P_1 and R_1 branches in stimulated emission spectra (see Fig. 3 of ref. 4). The parity splitting at $J = 3/2$ was determined to be 0.23 ± 0.03 cm^{-1}, which is approximately a factor of two smaller than expected based on the *ab initio* potential.

Using perturbation theory, Green and Lester[6] have shown that the parity doublets in the $j = 3/2$, $\omega = 3/2$, $P = 1/2$ bending levels are split apart in third order by a term proportional to the product of the Coriolis ($\boldsymbol{J} \cdot \boldsymbol{j}$), difference potential (V_2), and rotational decoupling ($\boldsymbol{j} \cdot \boldsymbol{s}$) terms divided by the appropriate energy denominators. The parity splitting in the $j = 3/2$, $\omega = 3/2$, $P = 1/2$ level was shown to have the following J-dependence

$$\Delta\nu_{P=1/2} = p(J + 1/2)$$

The magnitude of p was found to be directly related to the difference potential. As a result, the experimentally determined parity splitting for the 9.7 cm^{-1} band could be used to infer an average V_2 value of *ca.* 12 cm^{-1} in the region sampled by the first excited bend (centred at $R \approx 3.6$ Å, $\theta \approx 60°$). This value is smaller than expected based on the *ab initio* difference potential.[3]

The parity splitting for $j = 3/2$, $\omega = 3/2$ states with $|P| = 3/2$ arise in fifth order with the functional form for the splitting[6,7]

$$\Delta\nu_{P=3/2} = q(J - 1/2)(J + 1/2)(J + 3/2).$$

Dubernet *et al.*[7] have further shown that q could be related to the difference potential using a perturbative treatment. They also derived a relationship between q and p, evaluated the ratio $q/p = 8.99 \times 10^{-5}$ using molecular constants and potential parameters (based on the *ab initio* potential[3]), and showed that this ratio differs substantially from experimental findings.

In the light of this work[7,8] as summarized earlier by Dr. Dubernet and the suggestion by you that the P-doubling in the $P = 1/2$ state should be about three times larger than what we have observed,[4] we have re-analysed our experimental SEP spectra and find a best fit with $p = -0.155$ cm^{-1} and a rotor constant of 0.105 cm^{-1}. The negative sign on the parity splitting indicates that the + parity state is lower in energy. We emphasize that the SEP spectra were recorded using a Nd : YAG pumped dye laser with a laser resolution of 0.1 cm^{-1}.[4,5] Clearly, higher resolution spectra of the $P = 1/2$ band at 9.7 cm^{-1} would be desirable. This band should be observable by far-IR or near-IR spectroscopy.[2,9]

1 Y. Ohshima, M. Iida and Y. Endo, *J. Chem. Phys.*, 1991, **95**, 7001.
2 C. Chakravarty and D. C. Clary, *J. Chem. Phys.*, 1991, **94**, 4149.
3 A. Degli Esposti and H-J. Werner, *J. Chem. Phys.*, 1990, **93**, 3351.
4 M. T. Berry, M. R. Brustein, M. I. Lester, C. Chakravarty and D. C. Clary, *Chem. Phys. Lett.*, 1991, **178**, 301.
5 M. T. Berry, R. A. Loomis, L. C. Giancarlo and M. I. Lester, *J. Chem. Phys.*, 1992, **96**, 7890.
6 W. H. Green Jr. and M. I. Lester, *J. Chem. Phys.*, 1992, **96**, 2573.
7 M-L. Dubernet, P. A. Tuckey and J. M. Hutson, *Chem. Phys. Lett.*, 1992, **193**, 355.
8 M-L. Dubernet and J. M. Hutson, *J. Chem. Phys.*, 1993, **99**, 7477.
9 M-L. Dubernet, D. Flower and J. M. Hutson, *J. Chem. Phys.*, 1991, **94**, 7602.

Prof. Miller opened the discussion of Prof. Lester's paper: The rotational-state distributions resulting from vibrational predissociation of Ar–OH are quite surprising in view of the results obtained for more weakly bound complexes. The kinetic energy release in this system is clearly very large, which for a system such as Ar–HF would

result in a very long lifetime and population of the highest energetically allowed channel. The authors point out that the calculated distributions show much less translation energy, correlating with higher rotational states of the fragments. This is quite the opposite effect we observed previously in H_2–HF photodissociation, where the calculations gave distributions which were much less rotationally excited than those observed experimentally. The conclusion we made from this is that the anisotropy of the potential used in the calculation was too low, such that dissociation into the highest rotational states was inhibited. As a result of missing the contribution from these channels, the calculated lifetimes were longer than those observed experimentally. The situation is reversed in Ar–OH, where the anisotropy of the potential upon which the calculation is based is much larger than it should be. The question I have is, are the lifetimes and the rotational distributions correlated in the way discussed above and if not, how is this explained?

Prof. Lester and **Dr. Chakravarty** replied (in part communicated): In comparing experiment to theory for the vibrational predissociation of OH–Ar ($A\ ^2\Sigma^+$), three experimental observables should be considered: spectral shift of OH–Ar features in the OH A–X 1–0 *vs.* the 0–0 spectral region, predissociation linewidths (or lifetimes), and OH $A\ ^2\Sigma^+$ product rotational distributions. Each of these observables reflects different features of the underlying potential-energy surface and, taken together, provide a stringent test of the three-dimensional *ab initio* potential-energy surface $V(r, R, \theta)$ computed for the Ar–OH $A\ ^2\Sigma^+$ system.[1]

The computed binding energy (D_0) increases from 621 cm^{-1} (this value was reported at 597 cm^{-1} when the OH bond length, r, was fixed at 1.95 Å) to 824 cm^{-1} upon vibrational excitation of OH.[1,2] Experimentally, the binding energy of Ar to OH $A\ ^2\Sigma^+$ ($v = 0$) has been determined to be 742.9 cm^{-1} and increases by 32.5 cm^{-1} upon excitation of OH from the $v = 0$ to the $v = 1$ level.[3–5] The increase observed experimentally is seven times smaller than that predicted theoretically. The *ab initio* potential appears to overestimate the difference between $V_{11}(R, \theta)$ and $V_{00}(R, \theta)$ in terms of both well-depth and anisotropy. Here, $V_{v,v'}(R, \theta)$ represents vibrationally averaged matrix elements over the interaction potential $V(r, R, \theta)$.[1]

Since the predissociation rate has been shown to be strongly correlated with the square of the frequency shift in many atom–diatom systems,[6,7] one might expect that the computed vibrational predissociation lifetimes would be much too long (and the corresponding linewidths would be too small). Vibrational predissociation lifetimes were determined experimentally from the homogeneous contributions to the linewidths of OH–Ar features.[4] The lifetimes (τ_{vp}) were found to decrease rapidly with decreasing intermolecular stretching excitation (s) from 150 to *ca.* 20 ps for $s = 6$ to 3; thereafter little change in τ_{vp} was discerned. The computed linewidths follow the same trend, *i.e.* increasing linewidth with decreasing intermolecular stretching excitation, however the calculated linewidths are much smaller than the experimental linewidths by at least a factor of 30. This discrepancy between calculated and experimental linewidths may be due to the poor overlap of bound and scattering wavefunctions because of the relatively large difference in vibrationally averaged interaction potentials for the initial $V_{00}(R, \theta)$ and final $V_{11}(R, \theta)$ vibrational states.[1] Alternatively, the vibrational coupling term $V_{10}(R, \theta)$ may be too weak in the *ab initio* potential. Approximate calculations were performed to investigate the sensitivity of the predissociation linewidth to potential anisotropy.[1] The anisotropic terms in the Legendre expansions of the $V_{11}(R, \theta)$, $V_{10}(R, \theta)$, and $V_{00}(R, \theta)$ potentials were multiplied by a constant factor. Increasing the anisotropy by 10% increased the linewidth by factors of 1.5 to 3 and decreasing the anisotropy by 10% was found to decrease the linewidths by a similar amount. Note, however, that the approximate calculations did not distinguish between the various anisotropic terms and were meant to be indicators of the sensitivity to anisotropy.

In the work reported here we showed that the OH $A\,^2\Sigma^+$ products produced upon vibrational predissociation of OH–Ar had less rotational excitation than predicted theoretically. The theoretical calculations had predicted that OH product rotational distribution would peak near the energetic limit, $n = 11$ and 12.[1] The experimentally determined product rotational distributions reach a maximum at lower OH rotational levels, but still exhibit substantially more rotational excitation than that derived from the bending motion of the complex alone (see Fig. 5 of our paper). This suggests that the anisotropy of the vibrational coupling term $V_{10}(R, \theta)$ and/or the $V_{00}(R, \theta)$ exit channel is too strong. Spectroscopic studies have already shown that the angular dependence of the intermolecular potential correlating with OH $A\,^2\Sigma^+$ ($v = 0$)–Ar, $V_{00}(R, \theta)$, is too strong as evidenced by the much higher intermolecular frequencies computed for excited bending states than experimentally measured.[2]

Thus, comparison of experiment and theory is not as straightforward for OH–Ar ($A\,^2\Sigma^+$) as found for H_2–HF where both vibrational predissociation lifetimes and product rotational distributions indicated that the anisotropy of the potential used in the calculation was too low.[8] Hopefully, this new experimental data will prompt further calculations of the vibrational predissociation dynamics of OH–Ar ($A\,^2\Sigma^+$) on more realistic potential-energy surfaces.

1 C. Chakravarty, D. C. Clary, A. Degli Esposti and H-J. Werner, *J. Chem. Phys.*, 1991, **95**, 8149.
2 C. Chakravarty, D. C. Clary, A. Degli Esposti and H-J. Werner, *J. Chem. Phys.*, 1990, **93**, 3367.
3 M. I. Lester, R. A. Loomis, L. C. Giancarlo and M. T. Berry, *J. Chem. Phys.*, 1993, **98**, 9320.
4 M. T. Berry, M. R. Brustein and M. I. Lester, *J. Chem. Phys.*, 1990, **92**, 6469; 1989, **90**, 5878.
5 L. C. Giancarlo, R. W. Randall, S. E. Choi and M. I. Lester, *J. Chem. Phys.*, 1994, **101**, 2914.
6 R. E. Miller, *Science*, 1988, **86**, 507.
7 R. J. LeRoy, M. R. Davies and M. E. Lam, *J. Phys. Chem.*, 1981, **95**, 2167.
8 E. J. Bohac and R. E. Miller, *J. Chem. Phys.*, 1993, **98**, 2604.

Prof. Bačić said: It is interesting that the linewidths in the vibrational predissociation (VP) of Ar–OH, calculated by you, are smaller than the experimental results by more than an order of magnitude, while the calculated OH rotational state distribution peaks at higher j states than those seen experimentally. In the VP of H_2HF studied by us,[1] the calculated VP linewidth was also much narrower than the experimental one.[2] However, in this case the final-state rotational distribution showed much less rotational excitation of H_2 and HF fragments than the experimental distribution.[2] Consequently the fact that the calculated VP lifetime was much longer than the experimental one could be related to insufficient angular anisotropy of the potential at small H_2–HF distances. In contrast, the anisotropy of the Ar–OH potential appears to be too high, suggesting that here the main problem may be too weak coupling between the inter- and intramolecular degrees of freedom.

1 D. H. Zhang, J. Z. H. Zhang and Z. Bačić, *J. Chem. Phys.*, 1992, **97**, 3149.
2 E. J. Bohas and R. E. Miller, *J. Chem. Phys.*, 1993, **98**, 2604.

Dr. Chakravarty replied: It would appear that inaccuracies in the potential regarding both the anisotropy and the dependence of the Van der Waals potential on the intramolecular vibrational coordinate can lead to longer calculated lifetimes relative to experiment. It seems that the *ab initio* potential used for the Σ state of Ar–OH overestimates the difference in the vibrationally averaged intermolecular potential for the $v = 0$ and $v = 1$ levels leading to poor overlap of initial and final wavefunctions belonging to the two vibrational manifolds. For this system it may also be necessary to go beyond the golden rule approximation and incorporate the effects of higher vibrational levels.

Dr. Gray said: In relation to the VP work on ArOH described in the paper presented by Prof. Lester, I wish to comment that a very similar discrepancy between theoretical and experimental rotational product distributions occurs in the electronic

predissociation (due to the Renner–Teller effect) of HCO: HCO* → H + CO(j).[1] HCO* denotes an electronically (and rovibrationally) excited state, and H + CO(j) correlate with the ground electronic state. A time-dependent picture is useful for understanding the dynamics. Wave-packet amplitude is created at short times on the lower potential surface *via* electronically non-adiabatic coupling. This amplitude is localized in the collinear nuclear geometry region of the lower surface. Decay constants are mostly determined through this short-time process. The subsequent, essentially electronically adiabatic time-evolution of the amplitude on the lower surface determines the CO rotational product distribution.[1] It turns out that the wave-packet amplitude is created initially in a region of relatively high potential energy on the lower surface, and as the system bends from the collinear geometry, the amplitude descends a hill and thus picks up a lot of rotational kinetic energy. The theoretical hill is too high by at least 10%, and too much rotational kinetic energy is picked up. Hence the theoretical rotational product distributions are too hot and narrow in comparison with experiment. I wonder if a similar explanation could at least partly explain the results noted by Lester. VP is similar to electronic predissociation: short-time dynamics should determine the form of the wave-packet amplitude associated with a vibrational transition in the interaction region.[2] This amplitude should then evolve in a vibrationally adiabatic manner to form the relevant rotational product distributions. However, the intramolecular coupling responsible for the initial vibrational change is related to the derivative of the potential with respect to the coordinate associated with the relevant vibrational quantum number.[2] This function is probably not as localized, when viewed as a function of bending angle, as the analogous electronic predissociation case and so the initial vibrational transition itself may not only determine the decay constants, but also bias the rotational distributions before any subsequent vibrationally adiabatic time-evolution.

1 E. M. Goldfield, S. K. Gray and L. B. Harding, *J. Chem. Phys.*, 1993, **99**, 5812.
2 S. K. Gray and C. E. Wozny, *J. Chem. Phys.*, 1991, **94**, 2817.

Prof. Klemperer addressed Prof. Heaven and Prof. Lester: In comparing theory with experiment, one is concerned with both the possible inadequacies of experiments as well as those of theory. Is there any chance that the OH rotational distribution has been collisionally relaxed from the theoretically expected high J?

Prof. Heaven responded: There are two apparent discrepancies between theory and experiment for the vibrational predissociation of OH/D(A)–Ar. As noted, the rotational distributions measured for the OH(A) fragments are significantly cooler than the theoretical predictions of Chakravarty *et al.*[1] In addition, the measured and calculated predissociation rates differ by a factor of roughly 100. Prof. Lester notes that it is unlikely that the observed rotational distributions were modified by collisional relaxation. The experimental predissociation rates also appear to be secure.[2,3] We recently investigated[3] the linewidths of OH(A, $v = 1$)–Ar and OD(A, $v = 1$)–Ar at a resolution of 0.03 cm^{-1}. The rates obtained for OH(A, $v = 1$)–Ar were in agreement with the results of Berry *et al.*[2] Predissociation rates for OD(A, $v = 1$)–Ar had not been measured previously. They were a factor of two slower than the corresponding rates for OH(A, $v = 1$)–Ar.

Chakravarty *et al.*[1] calculated predissociation rates and final-state distributions using the Fermi golden rule approximation. The potential-energy surface used was obtained by fitting to a set of *ab initio* data points. Clearly, this surface was the most uncertain (and most critical) element in these calculations. Since the work of Chakravarty *et al.*,[1] a three-dimensional potential-energy surface has been derived from spectroscopic data by Schnupf *et al.*[4] Golden rule calculations that employed this potential also underestimated the predissociation rates.[5] However, in construction of the three-dimensional surface[4] it was assumed that the equilibrium internuclear distance [$R_e(\gamma)$] was not changed by vibrational excitation of OH(A). Reducing $R_e(\gamma = 0)$ for

OH(A, $v = 1$)–Ar, relative to OH(A, $v = 0$)–Ar, dramatically increased the calculated predissociation rates. Preliminary calculations[5] showed that reasonable agreement with the experimental rates could be obtained by contracting $R_e(\gamma = 0)$ by 0.06 Å. This change is permissible within the experimental uncertainties of the OH(A, $v = 1$)–Ar rotational constants.

We conclude that there is no serious disagreement between theory and experiment concerning the predissociation dynamics of OH(A)–Ar. Past problems stem from the reliance on *ab initio* potentials.

1 C. Chakravarty, D. C. Clary, A. Degli Esposti and H-J. Werner, *J. Chem. Phys.*, 1991, **95**, 8149.
2 M. T. Berry, M. R. Brustein and M. I. Lester, *J. Chem. Phys.*, 1990, **92**, 6469.
3 M. C. Heaven, *J. Phys. Chem.*, 1993, **97**, 8567.
4 U. Schnupf, J. M. Bowman and M. C. Heaven, *Chem. Phys. Lett.*, 1992, **189**, 487.
5 U. Schnupf, W. H. Basinger and M. C. Heaven, work in progress.

Prof. Lester also replied to Prof. Klemperer: In order to answer your question, let me elaborate on some of the details of our experimental methods.[1] We have determined the product-state distributions of the OH A $^2\Sigma^+$ fragments by using a novel variation of stimulated emission pumping. For these experiments, a frequency-doubled Nd : YAG-pumped dye laser (pump) is used to excite OH–Ar to a metastable intermolecular level supported by OH A $^2\Sigma^+$ ($v = 1$)–Ar potential. After a 200 ns delay, a collinear, counter-propagating XeCl-pumped dye laser (probe) is introduced to probe the nascent OH fragments by inducing downward transitions on OH A $\rightarrow$ X 0 $\rightarrow$ 1 transitions. When the probe laser is tuned to a downward transition originating from an OH A $^2\Sigma^+$ rotational level populated in the predissociation process, this laser removes population from that OH excited state rotational level *via* stimulated emission and, thus, decreases the spontaneous fluorescence from that level. Thus, a 'dip' in the spectrum results.

We have shortened the delay between the pump and probe lasers to 50 ns and observed the same product rotational distribution for the OH A $^2\Sigma^+$ fragments. We have also collected and dispersed the fluorescence ($\tau_{rad} \approx 700$ ns)[2] from the OH products[3,4] and found a similar product rotational distribution as that obtained by the stimulated emission pumping technique. The comparison with dispersed fluorescence spectra is only qualitative, as we are limited in our ability to determine the OH rotational distribution by the resolution of the monochromator used (*ca.* 60 cm^{-1}).

The rate of rotational transfer out of a given rotational level of OH A $^2\Sigma^+$ ($v = 0$) by Ar has been determined by Lengel and Crosley[5] to be 3 Torr^{-1} τ^{-1} (at 300 K) for $n = 4$, where τ is the radiative lifetime of OH.[2] In the 200 ns delay between pump and probe lasers, the rotational transfer rate becomes 0.9 Torr^{-1}. Assuming that the effective pressure of Ar carrier gas is less than 0.1 Torr at 40 nozzle diameters downstream of the nozzle (60 psi backing pressure, 300 μm nozzle diameter), then a simple kinetic analysis shows that $\leqslant 10\%$ of the OH A $^2\Sigma^+$ ($v = 0$, n) molecules may undergo rotational relaxation prior to being probed.

We see no evidence for rotational relaxation of the OH A $^2\Sigma^+$ ($n = 0$, n) products at low n and expect the probability of rotational relaxation to be even smaller for the higher rotational levels produced upon vibrational predissociation of OH–Ar by virtue of the increased energy spacing between rotational levels as n increases.

1 L. C. Giancarlo, R. W. Randall, S. E Choi and M. I. Lester, *J. Chem. Phys.*, in the press.
2 K. R. German, *J. Chem. Phys.*, 1975, **63**, 5252.
3 M. T. Berry, M. R. Brustein and M. I. Lester, *J. Chem. Phys.*, 1989, **90**, 5878.
4 M. T. Berry, M. R. Brustein and M. I. Lester, *J. Chem. Phys.*, 1990, **92**, 6469.
5 R. K. Lengel and D. R. Crosley, *J. Chem. Phys.*, 1977, **67**, 2085.

Dr. Ernesti communicated: Rotational rainbows are prominent features in rotationally inelastic differential cross-sections.[1,2,3] The relative transition probabilities discussed

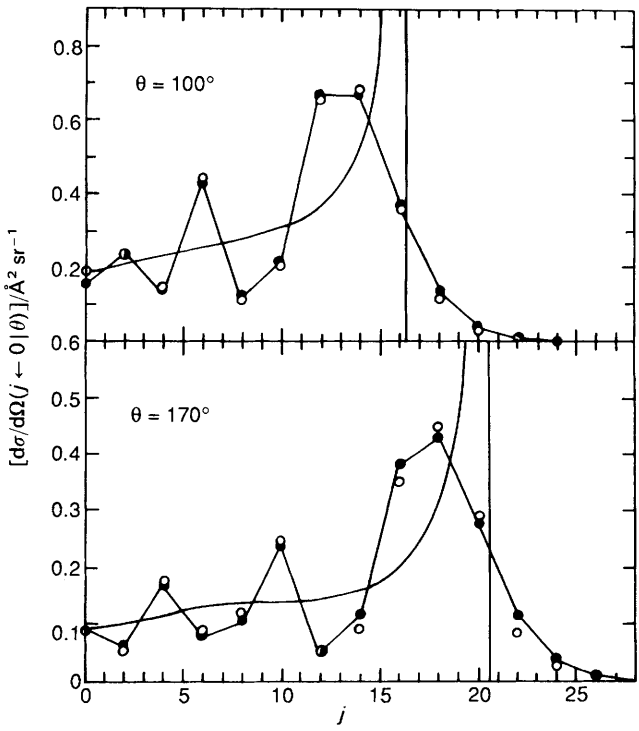

Fig. 2 Differential cross-sections for rotational transitions $0 \rightarrow j$ for He–Na_2 collisions at 100 meV. Quantum results (●) are compared with semiclassical approximations (○) and classical distributions (——). (Adapted from ref. 4)

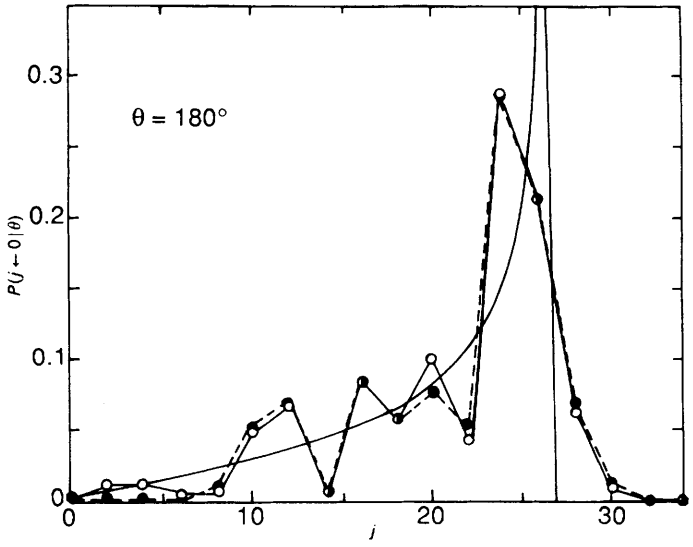

Fig. 3 Rotational transition probabilities $P(j \leftarrow 0 \mid \theta)$ for electron–Na_2 scattering at an energy of 300 eV and backward scattering. Close-coupling quantum computations (●) are compared with results from a two-centre spectator model (○). Also shown is the classical probability distribution (——). (Adapted from ref. 5.)

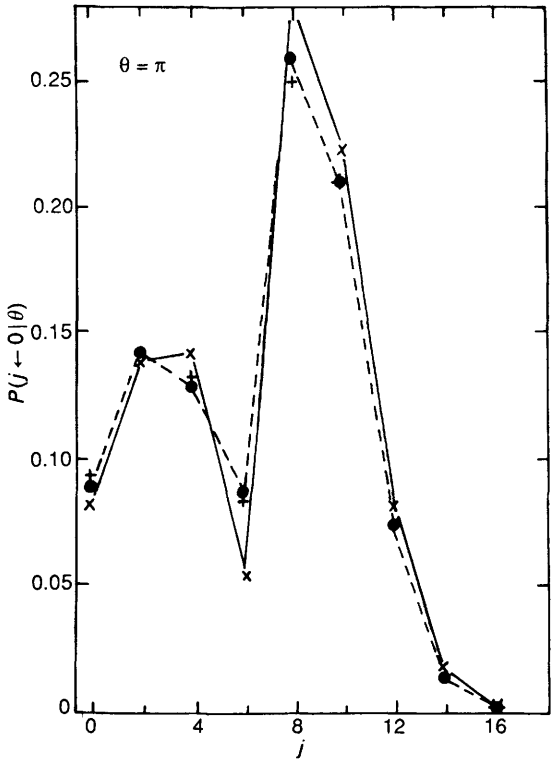

Fig. 4 Rotational transition probabilities $P(j \leftarrow 0 \mid \theta)$ for Coulomb excitation of ^{238}U colliding with ^{84}Kr at an energy of 300 MeV. Quantum results (●) are compared with semiclassical approximations; (+) De Boer and Winther, (×) 'Uniform semiclassical approximation'. (Adapted from ref. 6.)

by Lester *et al.* in Fig. 5 might be analysed in terms of rainbow effects. For comparison with Fig. 5, in Fig. 2–4 typical rotational rainbow distributions for the excitation from the ground state at fixed scattering angle θ are shown, ranging from molecular to nuclear scattering. Fig. 2 was obtained for He–Na_2 collisions at 100 MeV, Fig. 3 for electron–Na_2 scattering at an impact energy of 300 eV,[5] and Fig. 4 for Coulomb excitation of ^{238}U colliding with ^{84}Kr at an energy of 300 meV.[6] In each of these cases a pronounced rainbow maximum can be found close to the singularity of the classical rainbows, which are only shown in your Fig. 2 and 3. For small final rotational quantum numbers, each distribution shows rainbow oscillations and on the other side of the maximum an exponential decrease.

My questions are: Since vibrational predissociation may be seen as a 'half collision', is it possible to analyse your Fig. 5 in terms of rotational rainbows? If yes, what information about the potential-energy surfaces does such an analysis provide?

1 H. J. Korsch and A. Ernesti, *J. Phys. B*, 1992, **25**, 3585.
2 A. S. Dickinson and D. Richards, *Adv. At. Mol. Phys.*, 1982, **18**, 165.
3 R. Schinke and J. M. Bowman, in *Molecular Collision Theory*, ed. J. M. Bowman, Springer, Berlin, 1983.
4 H. J. Korsch and R. Schinke, *J. Chem. Phys.*, 1980, **73**, 1222.
5 H. J. Korsch, H. D. Meyer and C. P. Shukla, *Z. Phys. D*, 1990, **15**, 227.
6 S. Levit, U. Smilanski and D. Pelte, *Phys. Lett. B*, 1974, **53**, 39.

Prof. Lester replied: You asked if it was possible to interpret the product rotational distribution following vibrational predissociation of OH–Ar ($A\,^2\Sigma^+$) in terms of rota-

tional rainbows. We have previously done such an analysis on the ICl–He system where the two maxima observed in the experimental ICl fragment rotational distribution could be attributed to rotational rainbows.[1] In this system, the rotational rainbows were indicative of a rotationally inelastic scattering process (half-collision) taking place as the He atom recoils from the ICl molecule. Quantum close-coupling calculations confirmed that the rotational excitation of the ICl product was due to the anisotropic intermolecular interaction between the separating fragments.[2]

We have performed the same type of analysis to determine if the OH $A\,^2\Sigma^+$ ($v = 0$) product rotational excitation following vibrational predissociation of OH–Ar ($A\,^2\Sigma^+$) can be ascribed to a rotationally inelastic half-collision between Ar and OH. The analysis utilizes the semi-classical theory introduced by Schinke for the photodissociation of stable triatomic molecules.[3] Vibrational predissociation is modelled as a two-step process: preparation of the complex on the dissociative surface followed by a rotationally inelastic half-collision. The second step was simulated by running exact classical trajectories on an *ab initio* potential-energy surface[4] for Ar–OH $A\,^2\Sigma^+$ ($v = 0$) at an energy of 2815 cm^{-1}, the energy available for rotational and translational excitation of the fragments upon vibrational predissociation from the OH–Ar (K, s, b) = (0, 5, 0) level. The resultant rotational excitation function exhibits peaks at 70° ($n = 8$), 110° ($n = 9$), and 140° ($n = 7$).[5] In full collisions between OH $A\,^2\Sigma^+$ and Ar at this collision energy, the peaks in the rotational excitation function would map into peaks in the OH $A\,^2\Sigma^+$ product rotational distribution at $n = 7$, 8, and 9, known as rotational rainbows. The initial bending wavefunction for the OH–Ar complex in the $A\,^2\Sigma^+$ state, however, is localized about 0° (linear O—H–Ar configuration)[6] and therefore does not access the regions of the potential-energy surface that lead to strong rotational excitation (without a strong angular dependence to the vibrational coupling term[2]). Rather, the rotational reflection principle[3] would predict low rotational excitation of the OH products, $n = 0$ and 1, which is not consistent with the experimental results.

1 R. L. Waterland, J. M. Skene and M. I. Lester, *J. Chem. Phys.*, 1988, **89**, 7277.
2 R. L. Waterland, M. I. Lester and N. Halberstadt, *J. Chem. Phys.*, 1990, **92**, 4261.
3 R. Schinke, *Photodissociation Dynamics*, Cambridge University Press, Cambridge, 1993.
4 A. Degli Esposti and H-J. Werner, *J. Chem. Phys.*, 1990, **93**, 3351.
5 L. C. Giancarlo and M. I. Lester, unpublished results.
6 C. Chakravarty, D. C. Clary, A. Degli Esposti and H-J. Werner, *J. Chem. Phys.*, 1990, **93**, 3367.

Dr. Howard said: Concerning studies on the microwave spectroscopy of open-shell Van der Waals molecules, I would like to present results on the complex NO–HF. The IR spectrum has been previously observed,[1] but the microwave spectrum provides added information.

The spectrum is complicated because of the combination of all of the following factors: (*a*) it is an asymmetric top Van der Waals complex; (*b*) it possesses electron spin and orbital angular momentum (NO is $^2\Pi$); (*c*) the free orbital motion is partially 'quenched' by the presence of HF; (*d*) there is extensive hyperfine structure (principally due to the interaction of the magnetic field associated with the spin and orbital angular momenta interacting with the nuclear spins of each of N, H and F nuclei.

We have observed approximately 30 hyperfine transitions associated with each rotational transition. These transitions have been fully assigned but the hyperfine structure is not completely analysed. However approximate hyperfine constants have been derived.

For clusters containing a molecule in a π state there are two potential surfaces, one of A′ symmetry corresponding to the π electron within the plane of the complex and the other of A″ symmetry. The IR spectrum gives rotational and electronic fine structure but is unable to distinguish the order of the A′ and A″ potentials and hence the sign of the barrier to orbital motion.

By comparison, the nitrogen hyperfine structure determined from the microwave spectrum is sensitive to the preferred orientation of the NO π^* electron. It shows that the π^* electron prefers to be in the plane of the complex (A′ curve lowest), presumably attracted to the HF by some form of hydrogen bending. By comparison the T-shaped Ar–NO complex has been shown to give the opposite result,[2] with the A″ curve lowest. We interpret this as being due to the increased repulsion between Ar and NO in the A′ state.

1 W. M. Fawzy, G. T. Fraser, J. T. Hougen and A. S. Pine, *J. Chem. Phys.*, 1990, **93**, 2992.
2 P. D. A. Mills, C. M. Western and B. J. Howard, *J. Phys. Chem.*, 1986, **90**, 4961.

Prof. Dagdigian and **Prof. Alexander** communicated: Dr. Howard has commented that the sign of the difference potential (V_{dif}) for a Van der Waals complex involving an open-shell diatom in a Π electronic state can be determined experimentally from an analysis of the hyperfine structure of rotational transitions, as illustrated through experiments on NO($X\,^2\Pi$)–HF by Dennis, Howard and Whitham.[1] We would like to point out that a similar determination can be carried out using a Π–Σ electronic transition, in particular for a complex of singlet spin multiplicity, provided that the reflection symmetry of the diatom Σ state ($\Sigma^{\pm}$) is known. This is illustrated by our work on the ArBH($X\,^1\Sigma^+$, $A\,^1\Pi$) complex. Radiative transitions from the ground bend–stretch ArBH($X\,^1\Sigma^+$) level are allowed to stretch levels supported by only the upper of the two $P = 0$ bender curves correlating with the BH ($A\,^1\Pi$), $j = 1$)–Ar asymptote.[2] This is consistent with a primarily negative V_{dif} (sign convention from Alexander[3]), as also derived from electronic structure calculations on ArBH.[4] If the sign of V_{dif} were switched to positive, then the symmetries of the $P = 0$ curves would be interchanged, and transitions would be observed to stretch levels supported by the lower $P = 0$ bender curve.

1 C. R. Dennis, B. J. Howard and C. J. Whitham, poster at this Discussion.
2 E. Hwang and P. J. Dagdigian, *J. Chem. Phys.*, 1994, **101**, 2903.
3 M. H. Alexander, *Chem. Phys.*, 1985, **92**, 337.
4 M. H. Alexander, S. Gregurick and P. J. Dagdigian, *J. Chem. Phys.*, 1994, **101**, 2887.

Dr. Hutson said: I would like to broaden the discussion of open-shell systems to include complexes formed from open-shell atoms and at the same time issue a challenge to the experimentalists here. There is a great deal of interest, both experimental and theoretical, in prototype chemical reactions such as

$$F + H_2 \rightarrow FH + H$$

$$Cl + HCl \rightarrow ClH + Cl$$

So far, most of the work on these systems has concentrated on the short-range region around the transition state. However, there are strong long-range forces that can act to orient the reacting species, and which will also result in the formation of Van der Waals complexes. Dubernet and I have investigated the patterns of energy levels that should be expected for a range of atom–molecule complexes containing open-shell atoms.[1] In addition, we have made detailed predictions for the Van der Waals energy levels of Cl–HCl,[2] in the hope of stimulating measurements of its spectrum. There are three different potential-energy surfaces for Cl–HCl correlating with Cl (P). Let us consider first what happens in the absence of spin–orbit coupling:

(i) For a linear Cl–H—Cl geometry, the atomic orbital angular momentum $l = 1$ is quantised along the intermolecular (z) axis with projection λ, giving $\sigma\,(p_z)$ and $\pi\,(p_x, p_y)$ electronic states. The π curve is strongly attractive for the linear geometry, because of the electrostatic interaction between the atomic quadrupole and the molecular dipole and quadrupole, while the σ state is repulsive.

(ii) For non-linear geometries, the π state splits into p_z (A′) and p_y (A″) components. The two A′ states (p_x, p_z) are mixed. There are thus three distinct potential surfaces.

The effects of spin–orbit coupling are crucial in understanding the Van der Waals energy levels. The spin–orbit splitting in Cl is 882 cm^{-1}, so that λ is not a good quantum number even for the linear geometry: instead, the atomic total angular momentum j_a is nearly conserved. The spin–orbit coupling thus mixes the different spin-free potential surfaces, so that all three of the spin-free surfaces contribute importantly to the Van der Waals states.

We have carried out calculations on Cl–HCl at several different levels of sophistication: (i) calculations of the bending vibronic levels, considering only the anisotropic potential and the spin–orbit coupling; (ii) helicity decoupling calculations including the intermolecular stretch but neglecting off-diagonal Coriolis matrix elements; (iii) full close-coupling calculations, including all the vibronic and rotational coupling.

The vibronic Hamiltonian of the Van der Waals complex is

$$-\frac{\hbar^2}{2\mu} R^{-1} \frac{\partial^2}{\partial R^2} R + H_{\text{atom}} + H_{\text{mol}} + \frac{\hbar^2 \hat{L}^2}{2\mu R^2} + V(R, \theta, \theta_a, \phi - \phi_a)$$

where $H_{\text{atom}} = \xi \hat{l} \cdot \hat{s}$ and $H_{\text{mol}} = bj(j + 1)$. We solve this using a basis set made up of:

(1) atomic spin–orbital functions labelled by l, s, j_a.

(2) HCl internal rotational functions (spherical harmonics up to $j = 10$).

(3) Total angular momentum functions for the end-over-end rotation.

(4) The radial (R) motion is handled by solving coupled differential equations,[3] using the BOUND program,[4] not with a basis set.

We model the Cl–HCl potential as[2]

$$V_{\text{Cl–HCl}}(R, \theta, \theta_a, \phi - \phi_a) = V_{\text{Ar–HCl}}(R, \theta) + V_{\text{Cl–Ar}}(R, \theta_a) - V_{\text{Ar–Ar}}(R) + V_{\text{elec}}(R, \theta, \theta_a, \phi - \phi_a)$$

where V_{elec} is the long-range electrostatic potential (R^{-4} and R^{-5}). All the component intermolecular potentials are accurately known.[5–7] The electrostatic terms make a very important contribution to the potential, and result in a Van der Waals well that is substantially deeper than for closed-shell atom–diatom systems such as Ar–HCl.

The bending levels calculated for states of Cl–HCl correlating with Cl atoms in $^2P_3$ and $^2P_{1/2}$ states are shown in Fig. 5. The states correlating with $^2P_{3/2}$ are much more strongly bound, and the internal rotation of HCl in the complex is fairly strongly hindered. The states correlating with $^2P_{1/2}$, on the other hand, are much more weakly bound and the HCl molecule undergoes nearly-free internal rotation. The difference arises because the $^2P_{1/2}$ state of Cl has no electric quadrupole moment, so that the important electrostatic terms in the potential have very little effect.

Our main predictions are as follows:

(i) Cl–HCl is relatively strongly bound for a Van der Waals molecule (binding energy 275 cm^{-1}). The binding energy might be large enough to allow spectroscopy in a bulk sample (as opposed to a jet).

(ii) The lowest microwave transitions are $J = \frac{3}{2} \rightarrow \frac{5}{2}$ transitions in the $P = \frac{3}{2}$ ground state, and should occur near 9.40 GHz.

(iii) Far-IR bending bands are predicted around 55 and 78 cm^{-1}.

(iv) The HCl fundamental of Cl–HCl is probably red-shifted from the HCl monomer band origin by 6 to 8 cm^{-1}. Mid-IR combination bands should occur about 55 and 78 cm^{-1} above this.

(v) Mid-IR bands correlating with the $^2P_{1/2} \leftarrow {}^2P_{3/2}$ transition of the Cl atom should also have significant intensity: they are predicted around 1060 cm^{-1}, about 180

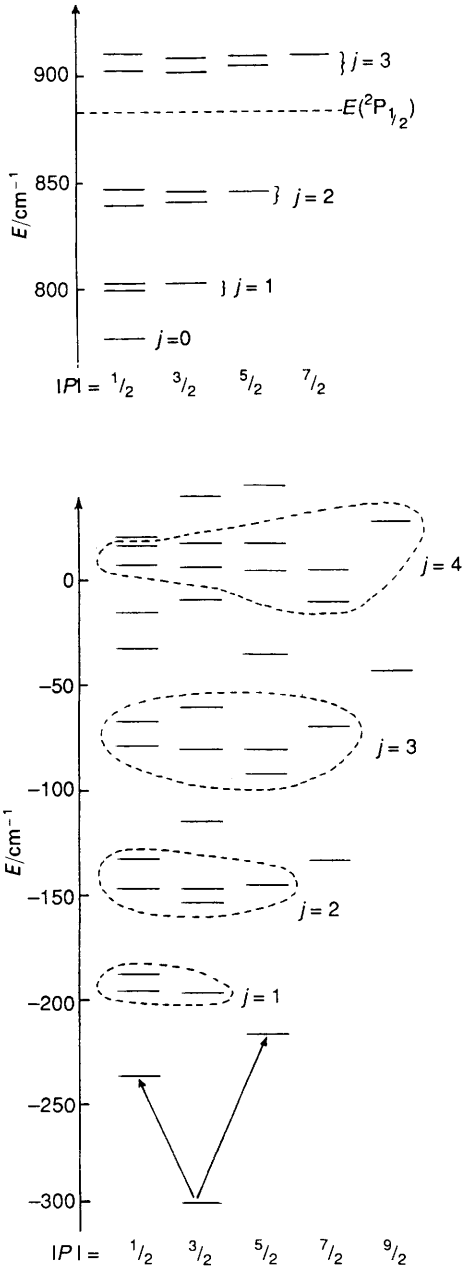

Fig. 5 Bending states for Cl–HCl at a fixed intermolecular distance, $R = 3.9$ Å

cm^{-1} blue-shifted from the atomic transition. The large shift occurs because the $^2P_{1/2}$ state of Cl has no electric quadrupole moment, as described above.

(vi) The levels correlating with $^2P_{1/2}$ can undergo electronic predissociation to form Cl ($^2P_{3/2}$) + HCl, but preliminary calculations suggest that this is very slow.

We would very much like to know if any of the experimentalists present see a prospect of forming Van der Waals complexes of this type and observing their energy levels.

If this is possible, it would provide a rich new source of information about the potential-energy surfaces for reactive systems.

1 M-L. Dubernet and J. M. Hutson, *J. Chem. Phys.*, 1994, **101**, 1939.
2 M-L. Dubernet and J. M. Hutson, *J. Phys. Chem.*, 1994, **98**, 5844.
3 For a review of the coupled-channel bound-state method, see J. M. Hutson, *Comput. Phys. Commun.*, in the press.
4 J. M. Hutson, BOUND computer code, version 5, distributed by Collaborative Computational Project No. 6 of the UK SERC, 1993. The BOUND program is available by anonymous ftp from Internet address krypton.dur.ac.uk.
5 R. A. Aziz and M. J. Slaman, *Mol. Phys.*, 1986, **58**, 679.
6 J. M. Hutson, *J. Phys. Chem.*, 1992, **96**, 4237.
7 V. Aquilanti, D. Cappelletti, V. Lorent, E. Luzzatti and F. Pirani, *J. Phys. Chem.*, 1993, **97**, 2063.

Prof. Wittig replied: Hutson's calculations of complexes like X–HX are very nice indeed. I would like to point out that we have shown that these radical–molecule complexes are produced efficiently by the ultraviolet photodissociation of the HX moiety within $(HX)_2$ complexes. See our comment concerning Prof. Klemperer's paper.

Dr. Krim said: In the present discussion there have been two reports of rotational predissociation in ArOH, ArCH of levels above the dissociation limit to the non-rotating fragments (OH, CH). These levels are on the half-collision side the analogues of rotational resonances described first by Levine *et al.*[1] and observed for NeHF.[2] The broadened lines corresponding to quasibound levels in effective potentials correlating with Ar–(OH, CH)$_{J>0}$ stand relatively isolated and can be easily identified.

On the contrary in HgN_2 that we have studied in the B state, there exists a domain in the dissociation continuum on which bands are superimposed. As transitions in the complex originate from the vibrational ground state, oscillations are not expected in the continuum. By spectroscopic means,[3] the onset of the continuum can be precisely determined and it corresponds in Fig. 6 to the sharp rise in intensity, going to higher frequencies. These bands are narrower on the low-energy side (2529 Å), and become broader on the high-energy side (2527 Å). We† have studied here their spectral and temporal behaviours. Lifetimes are measured by studying the dissociation in real time of the B state of HgN_2 complex. The experiment uses two picosecond laser pulses, pump–probe, as in our earlier comment. The first picosecond laser excites the complex from the ground state $HgN_2(X)$ to the first excited state in different regions of the quasi-continuum of the B state. The result of this excitation is analysed by the probe laser delayed from the pump pulse. The total mercury atomic fluorescence [Hg(^{3}D $\rightarrow$ ^{3}P$_2$)] is detected as a function of this delay time.

The dissociation product of the B state [Hg(^{3}P$_1$)] can be observed by tuning the wavelength of the probe laser at the mercury atomic transition [Hg(^{3}P$_1$–^{3}D$_1$)]. A transient signal, characteristic of the complex on its way to dissociation, can be detected by tuning the wavelength of the probe laser off resonance to the atomic line Hg(^{3}P$_1$–^{3}D$_1$).

As shown in Fig. 7 the onset of the product formation [Hg(^{3}P$_1$ + N$_2$)] is very slow and does not correspond to a direct fragmentation. The curve can be fitted with an exponential growth whose characteristic time varies depending upon the excess energy in the pump laser, with respect to the dissociation limit.

For position 1 at 2529 Å, the rise time is 5 ps while for position 2 at 2527 Å it amounts only to 2 ps. On the other hand the transients rise very sharply quite independently of the excitation but decay with the same time constant as the previous rise time. A long-lived transient species is therefore formed above the dissociation limit which corresponds to the excitation of quasi-bound states. The lifetime of such states cannot be

† L. Krim, B. Soep and J. P. Visticot.

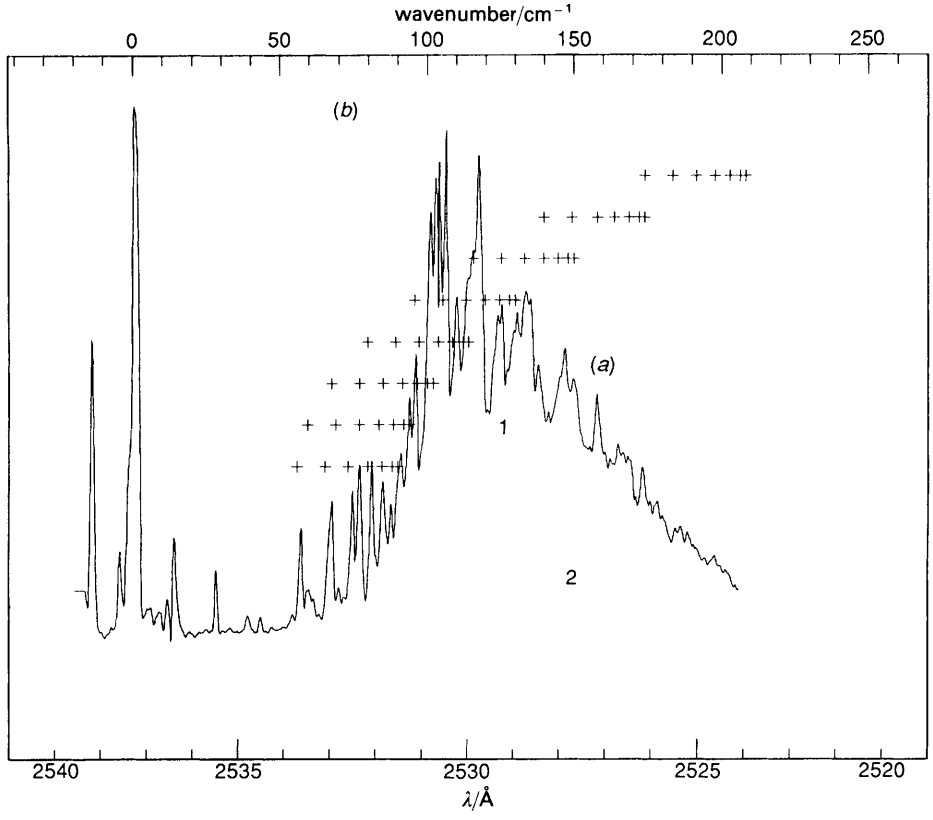

Fig. 6 (*a*) Fluorescence excitation spectrum of HgN_2. The zero on the wavenumber scale is set to the $Hg\ ^3P_1$ reference. The dissociation limit lies at 98 cm^{-1}. (*b*) The crosses indicate the calculated energy positions for different effective potentials correlating with $Hg + N_2(J)$, with 5 cm^{-1} anisotropy.

obtained through linewidth measurements since the lines are all inhomogeneous broadened.

Following Levine *et al.*[1] we have assigned the bound and the quasi-bound levels to the various HgN_2 (stretching) states that can be calculated in angle-averaged radial potentials, where the anisotropy is taken into account in averaged form.

This model can only be applied if the anisotropy of the potential is very small and, indeed, to show the existence of quasi-bound states within the $HgN_2(B)$ potential we have calculated classical trajectories, in order to find closed trajectories corresponding to quasi-bound states through each effective potential correlating to $Hg + N_2(J)$, see Fig. 8, the anisotropy cannot exceed 5 cm^{-1}.

The calculated level positions in effective potential corresponding respectively to $J = 0, 1, 2, 3, \ldots$ have been positioned above the spectrum in Fig. 6. One sees that in the bound portion of the spectrum each band can be unequivocally associated with a cluster of transitions correlating with $J = 0$–3. Above the dissociation limit a reasonable agreement persists. The ability to excite these quasi-free rotor states comes from the greater anisotropy in the $HgN_2(X)$ ground state more strongly bound and whose equilibrium distance is shorter by 1 Å.[3]

Hence we have identified in the dissociation continuum of the HgN_2 B state some resonances that relate to quasi-free rotation of the N_2 rigid rotor with respect to

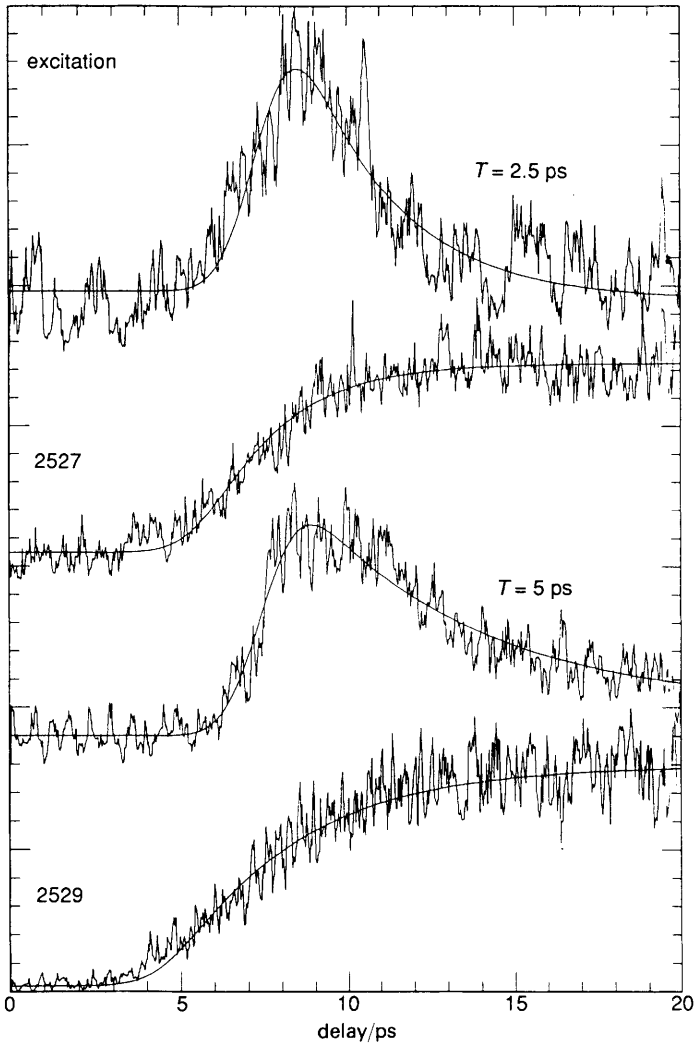

Fig. 7 Dissociation product probed at 3131 Å and transient signal probed at 3104 Å for two excitation wavelengths with the pump set on two maxima: top 2527 Å, position 2; bottom, 2529 Å, position 1 (see Fig. 6). The full lines indicates exponential fits of the data convoluted time constants for the rise and decay of the signals.

mercury. The dissociation arises from the anisotropy of the potential and the calculation of the rotational predissociation lifetime is in progress.

1 (*a*) R. D. Levine, *Acc. Chem. Res.*, 1970, **3**, 273; (*b*) R. D. Levine, B. R. Johnson, J. T. Muckerman and R. B. Bernstein, *J. Chem. Phys.*, 1968, **49**, 56.
2 D. J. Nesbitt, C. M. Lovejoy, T. G. Lindeman, S. V. ONeil and D. C. Clary, *J. Chem. Phys.*, 1989, **91**, 722.
3 K. Yamanouchi, S. Isogai, S. Tsuchiya, M. C. Duval, C. Jouvet, O. Benoist d'Azy and B. Soep, *J. Chem. Phys.*, 1988, **89**, 2975.

Prof. Vecchiocattivi said: When an atom–diatom Van der Waals molecule leads to a vibrational predissociation it can happen that the diatomic product is rotationally excited. In addition to examples reported in the present discussion,[1] I would mention

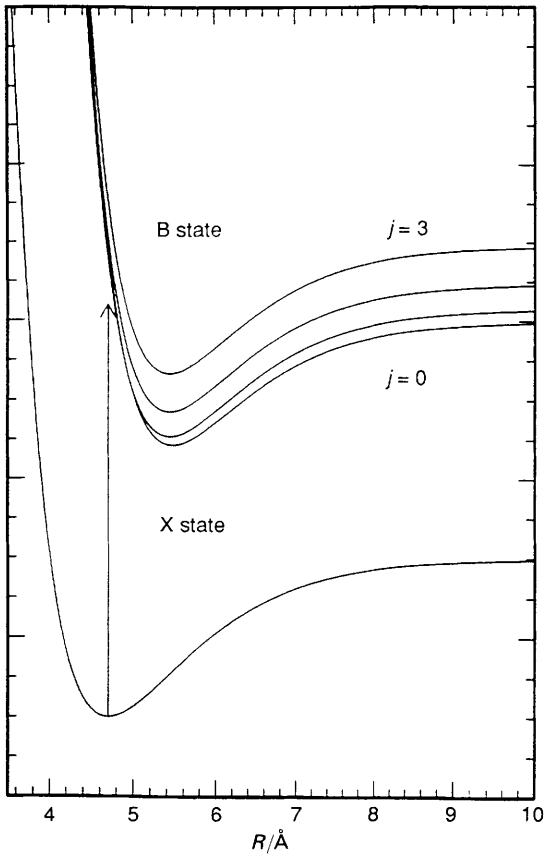

Fig. 8 Schematics of the potential-energy diagram for the X state and for the B state correlating with $Hg(^3P_1)$–$N_2(J)$

the case of the vibrational predissociation of $Ne–N_2^+$ presently studied in our laboratory.[2] This ionic Van der Waals molecule is produced by collisional autoionization[3] in a $Ne^*(^3P_{2,0})$–N_2 crossed-beam experiment where mass spectrometry is used to analyse and detect product ions. The autoionization leads to the formation of a $[Ne–N_2^+]$ complex which evolves dynamically to give $Ne + N_2^+$ and NeN_2^+. However in this latter Van der Waals ionic molecule, the N_2^+ subunit can be vibrationally excited leading therefore to a predissociation. The internal state distribution of the nascent $[Ne–N_2^+]$ complex is known after Hotop and co-workers[4] who measured the energy spectrum of the ejected electron. The final vibro-rotational distribution of N_2^+ ions has been measured by the use of the laser-induced fluorescence technique by Sonnenfroh and Leone.[5] Joining all this information together, one can easily realize that the predissociation of NeN_2^+ occurs with a rotational excitation of N_2^+.[2]

The problem in such a case is to recognize if this excitation, here as well as in other systems, is a simple consequence of the kinematics or is due to the dynamics of the process and therefore to potential-energy surface characteristics. Actually, when an atom–diatom complex dissociates, its total energy is redistributed in the translational, vibrational and rotational energy of the two fragments. On the other hand the total angular momentum of the complex, $\boldsymbol{L}$, is redistributed in the two vectors $\boldsymbol{j}$, the rotational angular momentum of the diatomic product, and $\boldsymbol{l}$, the orbital angular momen-

tum of the two fragments determined by the exit-channel impact parameter. The latter obviously produces a centrifugal barrier along the separation coordinate. This barrier is lower and more easily surmounted when l is small. However a small l implies a larger j, which means rotational excitation. This effect is more evident when the total energy is comparable with the largest possible centrifugal barrier.

Following this kinematic scheme, we have calculated the statistical expectation for the rotational distribution of N_2^+ product in the system under study. Practically, we have counted all the levels for the exit channels which fulfill the conservation of total energy and total angular momentum, excluding those which cannot surmount the centrifugal barrier. The result of the calculation clearly shows a strong rotational excitation. However, the experimental distribution appears shifted to lower energies with respect to the statistically expected one. Therefore the NeN_2^+ ion predissociation, following the $Ne^*(^3P_{2,0})$–N_2 collisional autoionization, occurs with a rotational excitation lower than expected from purely kinematics considerations, and this indicates that the rotational excitation is also determined by the dynamics of the process.

In conclusion, the statistical expected distribution based on simple kinematics considerations can be very useful for a primary assessment whether an experimental result about a predissociation process contains, or not, information about the potential-energy surface.

1 See M. I. Lester, S. E. Choi, L. C. Giancarlo and R. W. Randall, Faraday Discuss 1994, **97**, 365.
2 B. Brunetti, S. Falcinelli, S. Savini and F. Vecchiocattivi, to be published.
3 B. Brunetti and F. Vecchiocattivi, *Cluster Ions*, ed. C. Y. Ng, T. Baer and I. Powis, Wiley, New York, 1993, p. 359.
4 H. Hotop, personal communication.
5 D. M. Sonnenfroh and S. R. Leone, *Int. J. Mass Spectrom. Ion Processes*, 1973, **80**, 63.

Dr. Chakravarty opened the discussion of Dr. Syage's paper: Your results indicate that deviations from the Marcus-type parabolic dependence of reaction rate on the Gibbs energy differences in your system can be modelled including coupling of the tunnelling coordinate to the promoting mode. Is it possible, in these cluster systems, to use deviations from parabolic dependence to deduce which vibrational modes show significant coupling to the tunnelling mode? Are there examples where coupled vibrational modes act to reduce, rather than increase, the reaction rate relative to the value expected from the parabolic model.

Dr. Syage responded: Our understanding of departures from Marcus inverted-type behaviour comes mostly from electron-transfer studies in liquids. Models to explain inverted-region behaviour usually include a single vibrational mode that is known to undergo a change in equilibrium geometry and, therefore, is necessarily involved as an accepting mode coupled to the electron-transfer coordinate.[1] Including such a mode typically gives a dependence of rate on Gibbs energy that is consistent with experiment within the limits of the theory and the uncertainties of the experimental data. The role of vibrational coupling in proton transfer is more critical because the barrier penetration of a proton wavefunction is considerably less than that of an electron and, therefore, far more sensitive to other interactions. According to the model of proton tunnelling in clusters presented in my paper, it should be possible, based on the dependence of rate on reaction Gibbs energy to assign some important accepting modes in the product, or at least some estimate of the frequency ranges of importance. However, the usual methods of varying reaction Gibbs energy (*e.g.* cluster size, solvent type) necessarily change other properties (*e.g.* vibrational frequencies, structure) which may have important effects on rates. I think more experimental data are needed to refine the tunnelling models.

Aside from time-resolved methods, there may be other means to determine the vibrational modes that couple to the tunnelling coordinate. Since, these modes are populated

in the product, techniques that measure internal energy distributions could be fruitful. For excited-state proton transfer, one could use dispersed emission, stimulated emission and photoelectron spectroscopy. Because intramolecular vibrational redistribution will be fast in these systems, it may still be necessary to employ fast-time probing methods.

To answer your last question, it is possible for coupled vibrations to decrease tunnelling rate if one is at the peak of the Marcus curve (*i.e.* where reaction Gibbs energy equals the negative of the solvent reorganization energy). This is simply because coupled vibrations spread out the effective density of accepting modes, thereby diluting the effective density of states at the Gibbs energy corresponding to the Marcus peak. This effect is illustrated in Fig. 5 of my paper.

1 P. F. Barbara, G. C. Walker and T. P. Smith, *Science*, 1992, **256**, 975.

Prof. Donovan said: I would like to comment on the charge-transfer potentials and their perturbation by solvent molecules that you discuss. First, we have carried out numerous detailed studies of charge-transfer potentials[1,2] and find that whilst a simple Coulomb potential provides an accurate representation for charge separations greater than *ca.* 6 Å it fails substantially for smaller separations. The main difficulty is in estimating the repulsive part of the potential as this has a marked effect on the position of the minimum.

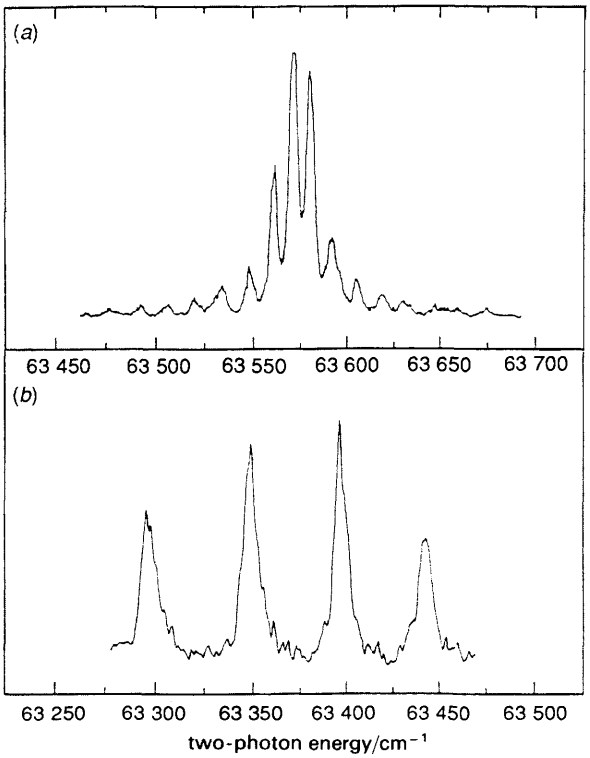

Fig. 9 Comparison of the (2 + 1) REMPI excitation spectra of I_2 and I_2–Ar. (*a*) The $v = 1$ level of the $[^2\Pi_{3/2}]_c$ 7s; 1g Rydberg state of I_2. The extensive ion-pair structure evident in the spectrum is indicative of strong Rydberg–ion-pair coupling. (*b*) Extended Van der Waals intermolecular vibrational progression built upon the same vibrational level ($v = 1$) of the $[^2\Pi_{3/2}]_c$ 7s; 1g Rydberg state of I_2–Ar. The lack of any resolved ion-pair structure indicates a decoupling of the Rydberg–ion-pair interaction as a result of the presence of the argon adduct.

Secondly, we have observed that charge-transfer states can be strongly perturbed by the Van der Waals bonding of even a single Ar atom.[3] Our observations are illustrated in Fig. 9 where (*a*) shows a transition to an electronic state of I_2, of mixed Rydberg–charge-transfer character. In the complex with Ar (*b*) the charge-transfer interaction has been removed and is replaced by a simple progression in the I_2–Ar stretch. We would expect the Van der Waals binding to differ substantially between the Rydberg and charge-transfer states and we interpret the loss of charge-transfer character to a substantial shift in the potential for this state. The shift in the Rydberg potential, induced by the presence of the Van der Waals bonded Ar atom, can be readily quantified by analysis of our spectroscopic data but further work will be needed to quantify the shift for the charge-transfer state.

1 K. P. Lawley and R. J. Donovan, *J. Chem. Soc., Faraday Trans.*, 1993, **89**, 1885.
2 P. J. Wilson, T. Ridley, K. P. Lawley and R. J. Donovan, *Chem. Phys.*, 1994, **182**, 355.
3 M. C. R. Cockett, J. G. Goode, K. P. Lawley and R. J. Donovan, *Chem. Phys. Lett.*, 1993, **214**, 27; M. C. R. Cockett, J. G. Goode, R. R. J. Maier, K. P. Lawley and R. J. Donovan, *J. Chem. Phys.*, 1994, **101**, 126.

Dr. Syage replied: I agree with Prof. Donovan that the repulsive part of a charge-transfer potential is more difficult to determine than the longer-range Coulomb part of the potential. A reasonable estimate of the repulsive potential is necessary for obtaining proper placement of the potential minima. The method we used to calculate the charge-transfer potentials has been described before.[1] The Coulombic contribution was calculated using literature values for charge distributions. Charge distributions for PhO were obtained from molecular orbital calculations by Taft and co-workers.[2] Charge densities for $H^+(NH_3)_n$ (up to $n = 4$) were calculated by Deakyne. The repulsive parameters were chosen to give an equilibrium internuclear separation of 1.8 Å for $O–N^+N$ based on a calculated distance for the ion-pair state of $PhOH–NH_3$.[4]

Prof. Donovan also notes that charge-transfer states can be strongly perturbed by Van der Waals bonding; he cites the example of I_2Ar from his work. That the charge-transfer states are strongly influenced by complexation is a main point of our work on PhOH solvated by NH_3 since it is the reason that one observes proton transfer in clusters and acid–base chemistry in general in condensed phases. The charge-transfer states, which exist at very high energies in isolated molecules, are stabilized enormously by polar molecules. For $PhOH–NH_3$ clusters, the PhOH charge-transfer potential that correlates to $PhO + H^+$ undergoes the following trend as a function of stepwise solvation by NH_3: a very large decrease in energy of the potential curve, a significant decrease in well-depth, and a moderate increase in the O–H internuclear distance.[1]

1 J. A. Syage and J. Steadman, *J. Chem. Phys.*, 1991, **95**, 2497.
2 A. Pross, L. Radom and R. W. Taft, *J. Am. Chem. Soc.*, 1980, **45**, 818.
3 C. A. Deakyne, *J. Phys. Chem.*, 1986, **90**, 6625.
4 A. Matsuyama and A. Imamura, *Bull. Chem. Soc. Jpn.*, 1972, **45**, 2196.

Dr. Müller–Dethlefs commented: Your results show that dynamic and reactive processes in hydrogen-bonded complexes can be followed by time-domain pump–probe experiments. For further investigations of proton tunnelling or proton transfer the application of ZEKE spectroscopy[1–3] offers new possibilities. Usually in such clusters the proton transfer is much more apparent in the cation than in the neutral species.[4] The cation thus offers a potential surface that is particularly suitable to project out the dynamics of the excited S_1 state. Selection of certain vibrations in the cation by ZEKE detection should, hence, allowing the probing of selective reaction coordinates in S_1. A problem that can arise is that a mass signature might be desirable in such ZEKE detection experiments. For this, a variant of the ZEKE method was proposed recently which relies on the detection of the ions produced by pulsed-field ionisation of ZEKE Rydberg

states (instead of electron detection).[5] The problem associated with mass-selected ZEKE measurements (termed 'mass analysed threshold ionisation', MATI[5]), however, has been the rather poor resolution and signal intensity compared with ZEKE measurements with electron detection.

Here we report the first high-resolution ZEKE measurements where both mass-selected ion and electron detection are performed in the same experiment, *i.e.* within a

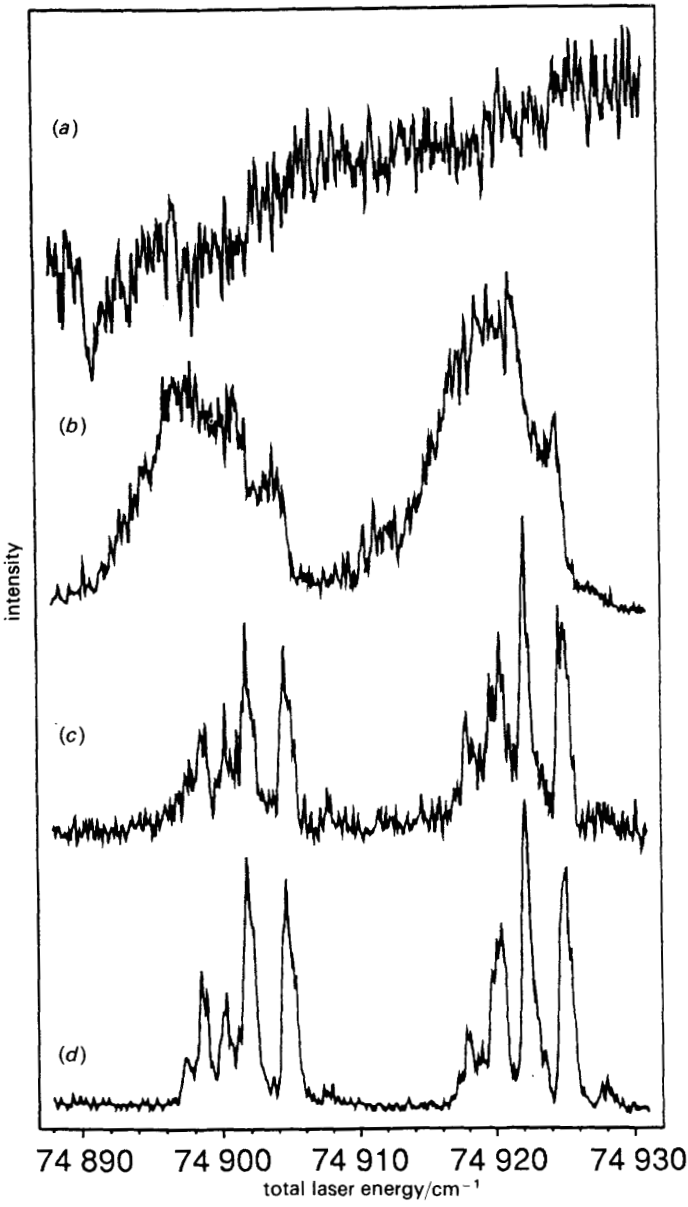

Fig. 10 (*a*) Photoionisation efficiency curve. (*b*) Low-resolution mass-selected ZEKE spectrum. (*c*) High-resolution mass-selected ZEKE spectrum. (*d*) High-resolution ZEKE spectrum with electron detection. All spectra were obtained for the ionising transition $D_0\ 6^1(3/2)$, $N^+, K^+ \leftarrow S_1\ 6^1\ J' = 4$, $K = 4$ of benzene. Reproduced with permission from ref. 6.

single laser scan.[6] This measurement is considered as a benchmark experiment in terms of resolution and signal intensity and was hence carried out for benzene and with rotational resolution. The results were obtained for the ionising transition D_0 6^1 (3/2), N^+, $K^+ \leftarrow S_1$ 6^1 $J' = 4$, $K = 4$ of benzene and are shown in Fig. 10. Fig. 10(*d*) shows the high-resolution ZEKE spectrum obtained with electron detection and should be compared to the mass-selected ZEKE spectrum [Fig. 10(*c*)]. Both spectra show essentially the same resolution; the MATI spectrum is lower in intensity by only a factor of two. Its full rotational resolution (0.6 cm^{-1}) must be contrasted with the low-resolution MATI spectrum obtained by applying just a high voltage pulse. For comparison, the total ion yield spectrum [Fig. 10(*a*)] is also shown; the PIE curve is essentially structureless.

In summary, this new high-resolution mass-selected ZEKE detection scheme should find applications for the study of reactive and dynamic processes in molecular clusters.

1 K. Müller-Dethlefs, M. Sander and E. W. Schlag, *Z. Naturforsch. A*, 1984, **39**, 1089.
2 G. Reiser, W. Habenicht, K. Müller-Dethlefs and E. W. Schlag, *Chem. Phys. Lett.*, 1988, **152**, 119.
3 K. Müller-Dethlefs and E. W. Schlag, *Annu. Rev. Phys. Chem.*, 1991, **42**, 109.
4 K. Müller-Dethlefs, O. Dopfer and T. G. Wright, *Chem. Rev.*, 1994, in the press and references therein.
5 L. Zhu and P. M. Johnson, *J. Chem. Phys.*, 1991, **94**, 5769.
6 H. J. Dietrich, R. Lindner and K. Müller-Dethlefs, *J. Chem. Phys.*, 1994, **101**, 3399.

Dr. Syage replied: The advances being made in mass-selected ZEKE (or MATI) should open many exciting avenues of research in cluster spectroscopy and dynamics. Dr. Müller-Dethlefs has reported a high-resolution variant of MATI. He has cited our time-dependent pump–probe experiments on hydrogen-bonded systems as a good case for applying ZEKE or MATI detection of the cluster ion for measuring details of the excited S_1 state dynamics. I might suggest another experiment that focuses on the properties of the cluster ions themselves. In earlier work, we determined potential-energy curves for the cluster ions showing a double minima (the barrier is due to a curve crossing).[1] We came to realize that this double-minima potential explained a long-standing issue in gas-phase ion molecule kinetics whereby certain reactions, those involving delocalized charge, could best be explained by a double-well reaction coordinate.[2] This premise could never be fully tested in gas-phase reactions because it was not possible to probe for the two different minima complexes. In recent work, we confirmed the double-minima potential for $PhOH^+ + NH_3 \rightarrow PhO + NH_4^+$ by selectively forming the two presumed complexes $PhOH^+$–$(NH_3)_n$ and PhO–$H^+(NH_3)_n$ by time-delayed ionization of reacting clusters.[1,3] Our evidence for the assignment is that when increasing the ionization energy the reactant ion complex would dissociate NH_3 whereas the product ion complex would dissociate PhO. MATI spectroscopy could provide vital structural information for the two complex forms and assess the role of stepwise solvation on the two complex forms. This effort would contribute not only to a greater understanding of cluster ion processes, but would make an important connection between cluster and gas-phase bimolecular chemistry.

1 J. Steadman and J. A. Syage, *J. Am. Chem. Soc.*, 1991, **113**, 6786.
2 C. R. Moylan and J. I. Brauman, *Annu. Rev. Phys. Chem.*, 1983, **34**, 187; P. B. Comita and J. I. Brauman, *Science*, 1985, **227**, 863.
3 J. A. Syage and J. Steadman, *J. Phys. Chem.*, 1992, **96**, 9606.

Prof. Simons said: Several contributors to this Discussion have addressed the question of overtone excitation in Van der Waals complexes; Prof. Wittig has commented on its utility as a means of cluster-size selection. Some years ago in the course of a study of H_2O_2 photodissociation at 248 nm, under jet-expansion conditions, Hodgson, Docker and I[1] discovered that expansion in Ar at stagnation pressures in the range 100–760 Torr, led to strong rotational cooling of the primary photofragments, OH ($v = 0$, N) and the development of a two-component Doppler profile in the rotationally relaxed levels.

These comprised equal contributions from a 'fast' component retaining the original recoil velocity (*ca.* 4 k ms^{-1}) and a 'slow' component. No such effect was seen in He expansions under similar conditions. The results are consistent with the dissociation of a linear dimer[2]

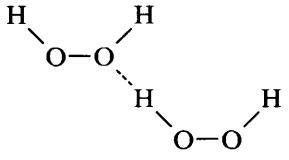

Recoil of the terminal OH fragment would be unhindered but the H-bonded fragment would be heavily relaxed as it scattered off the neighbouring peroxide molecule. When the same experiment was repeated under vibrationally mediated (VMP) conditions, employing two-photon excitation *via* the third overtone of the near local H—O stretching mode at *ca.* 750 nm, fragmentation to OH was completely suppressed in Ar.[3] One-photon vibrational predissociation from the fifth overtone was also suppressed. These experiments can be understood if IVR in the dimer leads to dissociation of the intermolecular H bond, rather than the intramolecular O—O bond. On the other hand, the VMP experiment should eventually be successful, if the energy of the second photon is increased until dissociation at the covalent bond is competitive with dissociation of the intermolecular bond. Given this happy event it should thus be possible to probe the consequences of initial vibrational excitation at three different types of O—H bond, either the terminal bond, the central donor or the acceptor bond.

1 M. P. Docker, A. Hodgson and J. P. Simons, unpublished work.
2 O. Mó, M. Yáñez, I. Rozas and J. Elguero, *Chem. Phys. Lett.*, 1994, **219**, 45.
3 M. Brouard, R. Mabbs and J. P. Simons, unpublished work.

Prof. Wittig said: The point has been raised about the variation of product detectability with interfragment distance in ultrafast measurements and about the $OH(A\,^2\Sigma)$ state that is produced in $H + N_2O$ collisions.

At short interfragment distances, the excited state used for LIF detection may be quenched by the nearby species. If quenching is efficient, as is known to be the case for $OH(A\,^2\Sigma) + N_2$ in collisional environments, one might see an induction period that reflects the need for the $OH–N_2$ distance to exceed a critical value before the OH product can be detected by LIF. In fact, Lester and co-workers have formed $OH–N_2$ complexes and find that many of the $A\,^2\Sigma$ levels cannot be used for LIF because of efficient quenching. It is possible that the quenching of $OH(A\,^2\Sigma)$ by N_2 is reactive, yielding $H + N_2O$ [as well as $OH(X\,^2\Pi) + N_2$]. This would be a nice experiment. Note that in our ultrafast experiment the OH and N_2 are travelling away from each other. It is not clear that quenching is independent of the direction of the relative velocity. Regardless, we measure OH build-up times $\leqslant 100$ fs, indicating a very fast reaction.

Prof. Wittig opened the discussion on Dr. Jouvet's paper: The photoinitiated decomposition of NO_2 occurs *via* a unimolecular reaction mechanism, which is quite different from direct photodissociation. The reactive NO_2 molecule contains a very large amount of vibrational excitation. Might this be important in your experiments. For example, could this cause higher-than-binary complexes to be favoured?

Dr. Jouvet replied: The point raised by Prof. Wittig is indeed very interesting. It is clear that because of indirect dissociation of NO_2, the vibrational predissociation (VP) of the $NO_2–C_2H_4$ complex can compete with the reactive process. However, only the reaction products are detected, thus only the complexes in which the reaction is faster

than the VP are observed. Therefore this will not perturb the internal energy distribution observed in the products.

In a large cluster $(NO_2)_n$–$(C_2H_4)_m$, VP can be hindered by a kind of cage effect which may be very efficient. This may favour the detection of reaction in clusters as compared to the reaction of binary complexes. In the case of reaction in clusters, one would expect some of the energy contained in the hot NO_2 molecule to be lost in the cluster either through vibrational redistribution within the cluster or through evaporation before the reactive event.

If clusters are the main source of the observed vinyloxyl radical, one should expect the reaction threshold observed in monitoring the vinyloxyl fluorescence as the NO_2 excitation laser is scanned, to be at higher energy than that observed by Kleinermanns and Luntz[1] in the crossed-beam experiment $[O(^3P) + C_2H_4]$. As shown in Fig. 11, the reactive threshold occurs at 394 nm whereas the dissociation threshold for NO_2 is 398.3 nm leading to the same activation energy (275 cm^{-1}) observed in the crossed-beam $O(^3P) + C_2H_4$ reaction. This clearly shows that no energy is dissipated in the cluster before the reaction.

Moreover, the experiments[2] of Frei and co-workers on NO_2–C_2H_4 in an Ar matrix have shown that the reaction can proceed on the singlet surface below the dissociation limit and on the triplet surface near the dissociative threshold of NO_2. One would then expect to observe the reaction below the threshold observed in the crossed beam, if the cage effect was the main reason for the observation of cold vinoxy.

In the insert of Fig. 11 one can see that the rotational contour, *i.e.* the internal rotational distribution of the vinyloxyl radical does not change when the excitation is set

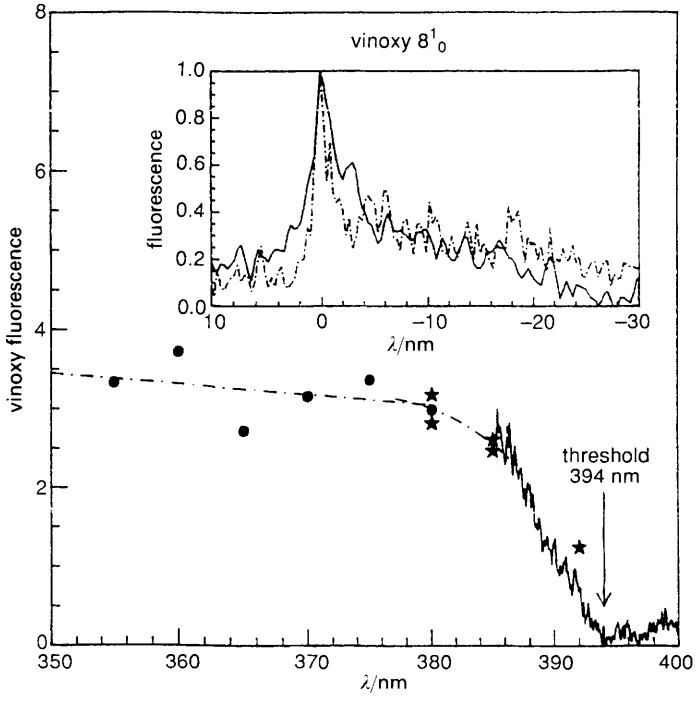

Fig. 11 Action spectrum of NO_2–C_2H_4 complex. The band head of the vinyloxyl radical is probed while the dissociation laser is scanned. The insert shows the rotational contour of the vinyloxyl product for two laser excitation wavelengths: (——) 385 nm and (· — ·) 355 nm.

at 355 or 385 nm. This is in agreement with the proposed interpretation of a late barrier in the exit channel.

1 K. Kleinermanns and A. C. Luntz, *J. Phys. Chem.*, 1981, **85**, 1966.
2 M. Nakata, K. Shibuya and H. Frei, *J. Phys. Chem.*, 1989, **93**, 7670.

Dr. Rühl commented: Photon-induced reactions within Van der Waals molecules often involve electronically excited states. The products can be specifically probed by laser-induced fluoresence, as shown in the papers presented by Prof. Wittig and Dr. Jouvet. However, this method works only if specific products are probed. We have applied an alternative approach for identification of all photoproducts including those with unknown spectroscopic properties: Photoreactions within clusters are initiated by pulsed UV-laser radiation which is followed by a pulse of vacuum ultraviolet (VUV) light. VUV laser radiation (E = 10.91 eV) ionises the photoproducts of reactive electronically excited states by one-photon absorption. The cations are subsequently separated by time-of-flight mass spectrometry.

Fig. 12 shows as a typical example that higher chlorine oxides such as Cl_2O_3 and Cl_3O_5 are formed *via* UV-photolysis at 359.55 nm ($OClO: \tilde{X}\,^2B_1 \rightarrow \tilde{A}\,^2A_2$) from chlorine dioxide aggregates $(OClO)_n$. These products have not been detected earlier by one- and two-colour REMPI spectroscopy. Fig. 12(*a*) shows that one-photon ionization with VUV laser radiation of neutral ground-state aggregates yields only $(OClO)_n^+$. Primary UV photolysis of OClO aggregates yields additional mass lines of higher chlorine oxides as well as ClO which is formed by predissociation of the isolated molecule [see Fig. 12(*b*)].

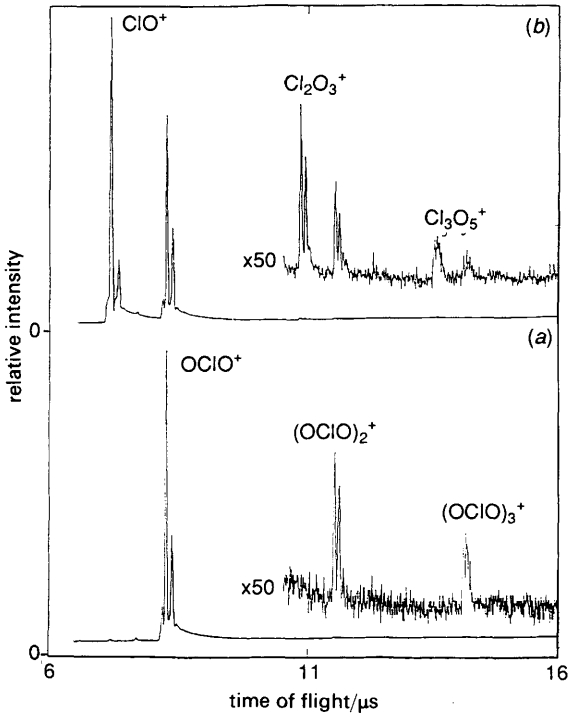

Fig. 12 Time-of-flight mass spectra of OClO aggregates: (*a*) ionisation with VUV laser radiation (E = 10.91 eV); (*b*) photolysis at 359.55 nm followed by ionization with 10.91 eV photons. Expansion conditions: 10% OClO in He, p_0 = 3.5 bar, T_0 = 300 K.

Prof. Bačić said: As in the case of gas-phase reaction dynamics, understanding of chemical reactions photoinduced in Van der Waals complexes will require close interaction between experiment and theory. The complex which appears to be among the most promising in this respect is H_2HF, and its isotopomers such as D_2HF. By photodissociating HF in the VdW complex, one can investigate the fundamental reactions of $H + H_2(D_2)$ and, possibly, $F + H_2$ in sterically constrained systems. This reaction has been studied intensely in the gas phase and there is excellent agreement between theory and experiments. Consequently, comparison with the reaction induced in the VdW complex should be particularly illuminating.

Dr. Jouvet said: Van der Waals complexes involving two reactive partners can be used as microscopic reactive systems with well defined geometry to study ionic reactions as in the case of ground-state or excited-state reactions, with the additional possibility of mass selection.

Nucleophilic substitution reactions in ionic halogenated benzene derivatives with various small molecules (water, methanol, ammonia) have been studied by Brutschy *et al.*[1,2] and our group.[3] These studies have been mainly performed using one-colour two-photon laser ionisation. The influence of the nature of the halogen (Cl or F), the relative position of the two substituents (in the case of dihalogenated benzene), the nature and the number of molecules of nucleophile on the reaction products has been evidenced.

We† present here new results on the *para*-fluorochlorobenzene–NH_3 complex using two complementary techniques: two-colour two-photon ionisation by lasers and one-photon ionisation by synchrotron radiation. New information on the reactivity have been obtained by varying the energy available for the reaction and performing kinetic measurements.

By ionising the *p*-FClB–NH_3 complex, three channels can be observed:

* (α) *p*-FClB–$NH_3^+ \rightarrow$ *p*FClB–NH_3^+ (non-reactive complex)
* (β) *p*-FClB–$NH_3^+ \rightarrow$ *p*-F anilinium + $Cl^\cdot$ (nucleophilic substitution)
* (γ) *p*-FClB–$NH_3^+ \rightarrow$ *p*-F aniline$^+$ + HCl (nucleophilic substitution)

Using two-colour experiments, we have measured the respective appearance thresholds of the product of channel (β) and (γ). For channel (β), this appearance threshold seems to correspond to the thermodynamical value of the exothermicity of the reaction.

We have also measured the rate of these two reactions channels: in the case of the *p*-F anilinium product, the reaction occurs on a tens of nanosecond timescale and in the case of *p*-F aniline$^+$, the reaction is slower: on a tens of microseconds timescale at threshold and the rate increases with the energy deposited in the ions.

It can be noticed, however, that in the case of laser experiments, there is no selectivity on the quantum state of the detected ions, *i.e.* ions with a large range of internal energies are formed, so that several processes appearing at different energies can be simultaneously observed [see Fig. 13(*a*) above the *F* anilinium appearance threshold, 9.09 eV, three channels are observed].

To overcome this difficulty, one-photon experiments using the synchrotron radiation of superACO in Orsay, coupled with the threshold photoelectron–photoion coincidences technique have been performed in the SAPHIRS set-up. By detecting the ions resulting from the chemical reaction in coincidence with threshold kinetic energy electrons, the internal energy of the system is well defined. We obtained the following results: (1) Above the *p*-F anilinium appearance threshold, we see only a fine peak corresponding to *p*-F anilinium [see Fig. 13(*b*)]. (2) Below this threshold, we see only the *p*-F aniline$^+$ mass peak, which is broad corresponding to a reaction time of 700 ns just below the *p*-F

† C. Jouvet, I. Dimicoli, C. Dedonder-Lardeux, S. Martrenchard-Barre, D. Solgadi, M. Richard-Viard and M. Vervloet.

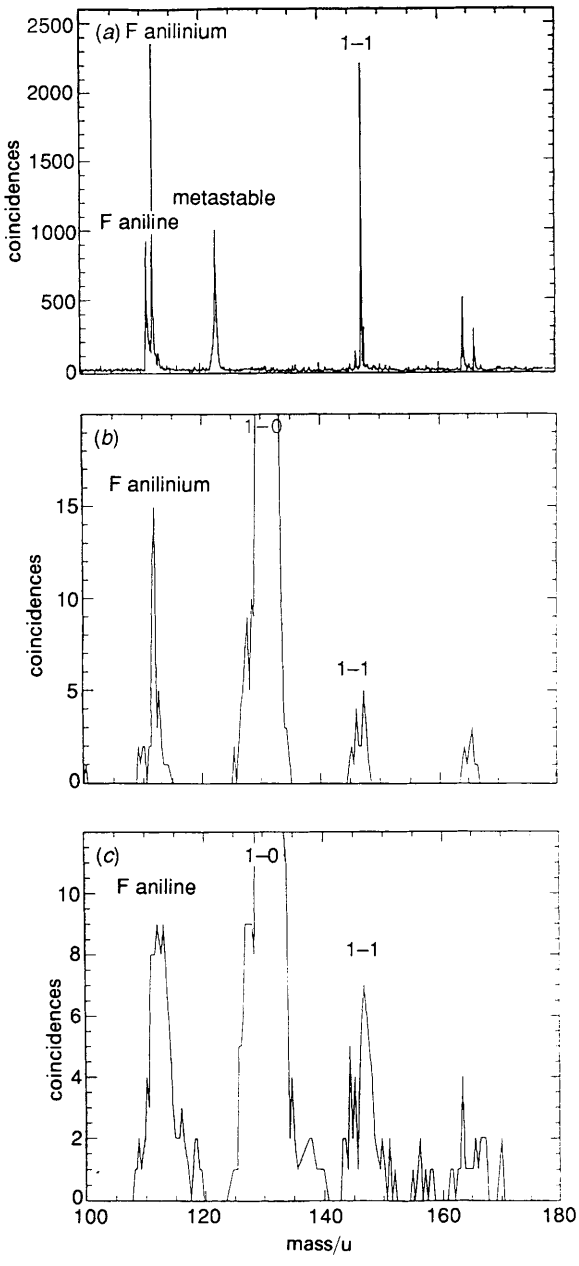

Fig. 13 Ionic products resulting from the reaction in the *p*-FClbenzene–NH_3^+ complex. (*a*) Laser experiment (9.1 eV): three mass peaks are simultaneously observed: 1–1 complex (α); *p*-F anilinium (β); *p*-F aniline$^+$ (γ): the reaction being on an ms timescale, two corresponding mass peaks are detected with delayed pulse field ionization: a 'stable' one which corresponds to reaction occurring between laser shot and extraction (here 500 ns) and a metastable one which corresponds to complex reacting in the first field-free region of the Reflectron MS synchrotron experiment (threshold photoelectron–photoion coincidences): (*b*) Ionization energy 9.09 eV, *p*-F anilinium mass peak, only the channel (β) is observed. (*c*) Ionization energy 9.08 eV, broad *p*-F aniline$^+$ mass peak.

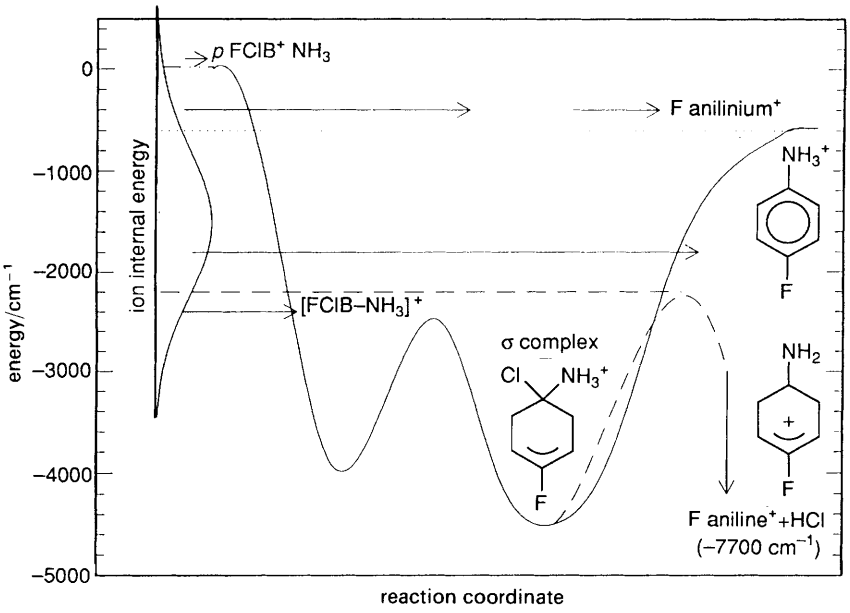

Fig. 14 Energy diagram for the nucleophilic substitution reaction. Reaction products are shown depending on the internal energy of the 1–1 complex. Energies are given with respect to the dissociation limit of the 1–1 ion and the internal energy distribution is modelled for the laser experiments. (——) Reaction coordinate for sigma complex formation; (– – –) reaction coordinate for *p*-F aniline$^+$ exit channel.

anilinium threshold [see Fig. 1(*c*)]. (3) Decreasing the energy again, only the 1–1 complex remained.

Comparison of the laser and synchrotron results leads us to propose the following mechanisms for the two reactive channels (β) and (γ) (see Fig. 14):

(1) *p*-F anilinium: formation of an addition complex, the sigma complex, as already proposed by Shaik and Pross[4] with a barrier to the reaction in the entrance channel lower than the exothermicity threshold.

(2) *p*-F aniline$^+$: we assume the existence of the same intermediate sigma complex. However, the exit channel, proton transfer from NH_3 to Cl in the sigma complex, is slower than the direct chlorine abstraction (microsecond timescale) so that channel (γ) is only observed when channel (β) is energetically closed (see Fig. 14).

Additional experiments on fluorobenzene, *meta*-fluorochlorobenzene–ammonia complexes and on larger clusters enable us to validate the previous assumptions.[5]

1 B. Brutschy, *J. Phys. Chem.*, 1990, **94**, 8637, and references therein.
2 C. Riehn, C. Lahmann and B. Brutschy, *J. Phys. Chem.*, 1992, **96**, 3626.
3 S. Martrenchard, C. Jouvet, C. Lardeux-Dedonder and D. Solgadi, *J. Phys. Chem.*, 1991, **95**, 9186.
4 S. S. Shaik and A. Pross, *J. Am. Chem. Soc.*, 1989, **111**, 4306.
5 S. Martrenchard-Barra, C. Jouvet, C. Dedonder-Lardeux and D. Solgadi, to be published.

Prof. Bréchignac said: There is one aspect of Van der Waals molecules which has not been discussed very much during these three days, although it was implicitly present in a few written papers and explicit in Prof. Knee's paper and in many discussions yesterday about ZEKE or resonant ionization spectroscopy. It is the shift of the ionization potential (E_i) induced by the binding of a partner on a parent molecule, in other words the degree of stabilization of the Van der Waals bond resulting from the ionization of the

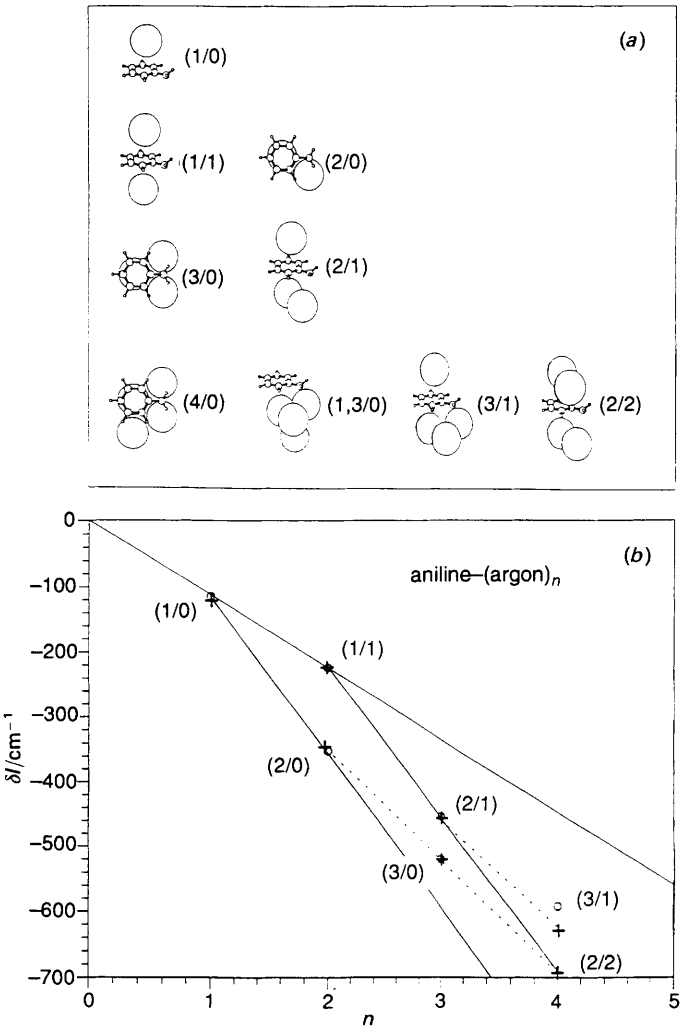

Fig. 15 (*a*) Geometrical configurations of the structural isomers of aniline–(argon)$_n$ clusters. (*b*) E_i shift values measured for these isomers; the straight lines correspond to the size-specific model.[1]

system. I think that this problem is far from being properly understood and is still a challenge for theoreticians. To take an example, the Van der Waals E_i shift for one argon atom attached to most of the aromatic molecules is very small: the average value is of the order of 100 cm^{-1} only, it hardly reaches 200 cm^{-1} in some cases, which is much less than the induction energy resulting from a positive charge in the π cloud and the argon polarizability. In fact these shifts depend much on the exact structure of the aromatic molecule, the presence of atoms with excess valence electrons seeming to favour larger values of the red shift. Even more precisely we have shown, by isomer selective measurements for aniline–(argon)$_n$ clusters,[1] that the value of the red shift induced by each argon atom depends in a non-trivial way on the nature of the binding site in which the atom sticks on the aromatic microsurface skeleton. This is illustrated in Fig. 15; the top panel recalls the structures of the various isomers, whose E_i shifts are plotted as a function of the number of the argon atoms in the bottom panel. Atoms binding next to the nitrogen lone pair induce larger shifts than the 'ring'-site atoms.

I wish to suggest that people think about this question which is, I believe, difficult to understand so far.

1 S. Douin, P. Hermine, P. Parneix and Ph. Bréchignac, *J. Chem. Phys.*, 1992, **97**, 2160.

Prof. Smith said: Dr. Jouvet and Prof. Wittig have provided us with nice examples of the elegant technique in which reagents for a bimolecular reaction are prepared by photodissociation of one component of a Van der Waals molecule. In this comment, I want to draw attention to other circumstances in which the long-range, attractive intermolecular forces which are our focus at this meeting play a role in bimolecular chemical reactions. In so doing, I should like to point out deficiencies in our knowledge of the long- and medium-range forces which act between potentially reactive species. A knowledge of these forces is necessary if the rates of chemical reactions between neutral species at ultra-low temperatures are to be successfully modelled and our ignorance of these forces presents what I believe to be an important challenge to theoreticians and experimentalists.

In order to explain this need, I must give you a brief account of some recent, and ongoing, experiments which are being conducted in a CRESU (Cinétique de Réactions en Ecoulement Supersonique Uniforme) apparatus[1] at the University of Rennes in a collaboration involving Bertrand Rowe, Ian Sims and others, as well as myself. In the CRESU apparatus, expansion of gas through a properly designed Laval nozzle produces downstream a supersonic flow of gas at relatively high uniform density (typically 10^{16}–10^{17} molecule cm^{-3}), and low and defined temperature (down to 13 K in our experiments[1]), in which there is a uniform, thermal collision density. In this medium, we determine rate constants for reactions of free radicals by the well established technique which uses pulsed laser photolysis to generate radicals and laser-induced fluorescence to observe their subsequent decay. In this way, we have already obtained rate constants for the reactions of CN (with O_2,[1] NH_3[1] and C_2 hydrocarbons[2]), of OH (with butenes,[3] HBr[4] and NO) and of CH (with D_2, O_2, NO and NH_3). In all cases, the experiments extend down as low as 25 K, and, for several reactions, rate constants have been measured at 13 K. It is important to note that these conditions access temperatures which are appreciably less than typical values of (ε/k_B), where ε is the Lennard-Jones well-depth.

A detailed understanding of our results requires a knowledge of the inter-reagent potentials, and their dependence on orientation and stereochemical factors, in the awkward range of separation where, as well as the limiting electrostatic or Van der Waals forces, chemical forces are starting to act. Two cases can be distinguished. For a number of reactions that we have studied, including CN + O_2[1] and CN + C_2H_2,[2] the rate constants increase monotonically as the temperature is lowered to values close to the Lennard-Jones collision rate constant, if allowance is made for any electronic degeneracy factors.

In this case, adiabatic capture theories[5] are likely to provide accurate estimates of the rate constants if sufficiently accurate representations are available of the potential-energy surface at large and fairly large separations of the reagents. The second case, exemplified by CN + C_2H_6, is even more interesting. The rate constant for this reaction increases, albeit quite slowly, as the temperature is raised above room temperature. However, the rate constant also increases strongly below *ca.* 100 K, reaching its highest observed value at 23 K.[2] These observations suggest that there can be no significant barrier to reaction along the minimum-energy path(s) leading from reagents to products (HCN + C_2H_5). We have suggested that the unusual temperature-dependence of the rate constant is a consequence of a change in collision dynamics. At temperatures where $T > (\varepsilon/k_B)$, collisions are predominantly direct and reaction only occurs if the collision energy exceeds the barrier to reaction for the particular orientation of the

reagents in the collisions. At lower temperatures, where $T < (\varepsilon/k_B)$, collisions become less direct and energised Van der Waals complexes may form allowing the reagents the opportunity to find the correct orientation for reaction to occur. Quantitative tests of such a hypothesis, again, require information about the Van der Waals interactions for such species and their orientation dependence.

1 (*a*) I. R. Sims, J-L. Queffelec, A. Defrance, C. Rebrion-Rowe, D. Travers, B. R. Rowe and I. W. M. Smith, *J. Chem. Phys.*, 1992, **97**, 8798; (*b*) I. R. Sims, J-L. Queffelec, A. Defrance, C. Rebrion-Rowe, D. Travers, P. Bocherel, B. R. Rowe and I. W. M. Smith, *J. Chem. Phys.*, 1994, **100**, 4229.
2 I. R. Sims, J-L. Queffelec, D. Travers, B. R. Rowe, L. B. Herbert, J. Karthauser and I. W. M. Smith, *Chem. Phys. Lett.*, 1993, **211**, 461.
3 I. R. Sims, P. Bocherel, A. Defrance, D. Travers, B. R. Rowe and I. W. M. Smith, *J. Chem. Soc. Faraday Trans.*, 1994, **90**, 1473.
4 I. R. Sims, I. W. M. Smith, D. C. Clary, P. Bocherel and B. R. Rowe, *J. Chem. Phys.*, 1994, **101**, 1748.
5 D. C. Clary, *Annu. Rev. Phys. Chem.*, 1990, **41**, 61.

Prof. Klemperer asked: In the low-temperature, high-expansion pressures regime is there the possibility that three-body collisions and/or the formation of long-lived complexes of the reactants are occurring? In this event the nature of the reaction could be significantly changed from the binary collision at lower expansion pressures.

Prof. Smith replied: We have considered carefully the possibility raised by Prof. Klemperer but several pieces of evidence clearly demonstrate that we are measuring the rate constants for bimolecular reactions between the radicals, which we produce by photolysis of a suitable precursor, and the second reagent, which is present in considerable excess over the radical but is still only a small fraction of the total gas mixture, rather than the three-body formation of a Van der Waals complex of these species. Before mentioning some of the relevant evidence, and indicating under what circumstances the formation of Van der Waals complexes can hamper our experiments (further details are given elsewhere[1]), it is worth emphasising that the expansions in our experiments are relatively mild: with the density decreasing by a factor of 10–100 from the reservoir to the low-temperature gas flow. Furthermore, the temperatures that are generated are not as low as those produced in the free-jet expansions that are widely used to create Van der Waals complexes for spectroscopic purposes.

To substantiate our contention that formation of stabilised radical–reagent Van der Waals complexes is unimportant in our experiments, I shall cite here three pieces of evidence. The first is that the measured rate constants for all the rate constants that we have measured, except those for OH + NO, show no dependence on total gas density. Actually, the magnitude of the measured rate constants for other reactions would require that, if association was responsible, the rate constants would have to be at, or close to their high-pressure limit. However, our measurements show that the radical–radical association reaction OH + NO is still far from its high-pressure limit under similar conditions, and radical–reagent complexes would surely associate much more slowly than OH + NO.

The second reason for rejecting significant formation of radical–reagent Van der Waals complexes is based on calculations of the equilibrium constants for the first dimer complex using statistical thermodynamics. Given the low partial pressure of the reagents, thermodynamics would only favour dimerisation to any degree at the lowest temperature of our measurements. In this respect, it is helpful that Van der Waals forces involving open-shell species are rarely significantly stronger than those for closed-shell molecules.

Paradoxically, our final reason for confidence also serves to demonstrate that the formation of Van der Waals complexes cannot be entirely ignored in our experiments. At 13 K, there are clear indications (see Fig. 5 in ref. 1) that O_2 starts to dimerise at the

highest concentrations that we have attempted to use. At these concentrations, the values of the observed CN decay constants (k_{1st}) no longer vary linearly with the concentration of O_2 over the complete range of O_2 concentrations. However, k_{1st} does increase linearly with $[O_2]$ over a sufficient range for the rate constant for CN + O_2 to be derived. These observations provide a guide to the rates of complex formation by gas-phase association in the ultra-cold gas, and show that this process is too slow to make a significant contribution to the rates of removal of free radicals under the conditions of our experiment.

1 I. R. Sims, J-L. Queffelec, A. Defrance, C. Rebrion-Rowe, D. Travers, P. Bocherel, B. R. Rowe and I. W. M. Smith, *J. Chem. Phys.*, 1994, **100**, 4229.